Summer 2010

Low cost passive dampers for highway traffic signs

Lea Ljumanovic
University of Iowa

LOW COST PASSIVE DAMPERS FOR

HIGHWAY TRAFFIC SIGNS

by

Lea Ljumanovic

A thesis submitted in partial fulfillment
of the requirements for the Master of
Science degree in Civil and Environmental Engineering
in the Graduate College of
The University of Iowa

July 2010

Thesis Supervisor: Assistant Professor Salam Rahmatalla

Graduate College
The University of Iowa
Iowa City, Iowa

CERTIFICATE OF APPROVAL

MASTER'S THESIS

This is to certify that the Master's thesis of

Lea Ljumanovic

has been approved by the Examining Committee
for the thesis requirement for the Master of Science
degree in Civil and Environmental Engineering at the July 2010 graduation.

Thesis Committee:

Salam Rahmatalla, Thesis Supervisor

Colby Swan

Shaoping Xiao

In loving memory of Dragan Loncar

ACKNOWLEDGMENTS

Special thank you to Professor Salam Rahmatalla for helping me with starting and completing this project, and for helping me stay motivated along the way. Special acknowledgments are extended to Dean Macken from the Engineering shop for helping with the construction of the model. In addition, recognition is given to Kyle Hudson for helping with the experiments. Acknowledgments are extended to Professor Colby Swan and Professor Shaoping Xiao for serving on the thesis committee. Finally I would like to extend deepest thank you to my mom, sister, and uncle for their unlimited support during this time.

TABLE OF CONTENTS

LIST OF TABLES

LIST OF FIGURES

CHAPTER I
INTRODUCTION AND BACKGROUND

1.1 Introduction

Highway signs are one of the most vital objects in the transportation infrastructure. There are tens of thousands of signs in the United States alone, not counting simple sign supports. [5] These signs have a limited lifetime because they have a tendency to fail under several live and dead load, wind loads and ice loads. High winds and vibration caused by traffic are the major cause of failure to highway signs. Vibration induces complex form of high magnitude signals that tend to provoke significant degree of relative motion between the top and the bottom of the structures. This results in a considerable amount of inertial forces that cause a fatigue type cracks that grow with time. In general, failure of highway signs are results of bending, shear and fatigue stresses. Types of structures that experience these failures include sign structures such as straight and cantilever members, utility poles (Figure 1) and others.

Figure 1: Broken pole

1.2 Loading

The most significant causes of damage for the highway signs are the forces generated form gusty wind, wind from speeding traffics, and random vibration signals from the ground due to traffic and other natural sources. Unless for hurricanes situations and gusty wind, the wind loads might not always be significant enough to break the structure; however, they play an important factor in the fatigue failure due to cyclic loading. The ground motion signal is very important in states that are earthquake prone such as California and the Golden Gate Bridge. Figure 2 illustrates the two most common loads that simple sign structures experience.

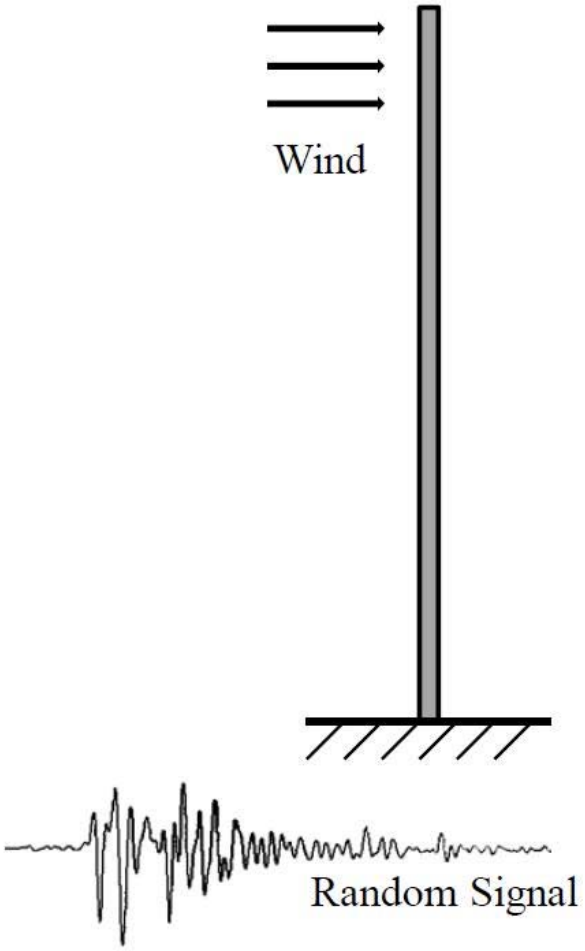

Figure 2: Loading on the sign structure

1.2.1 Wind

It is well known that wind is one of the most significant damaging factors to the highway signs. The wind can generate a tremendous amount of forces especially during hurricanes scenarios; additionally, its speed and direction can varies significantly with geometrical regions as shown in Figure 3. Besides the wind that is naturally generated, vehicles passing by the signs can create gust of wind that may also result in sign failures.

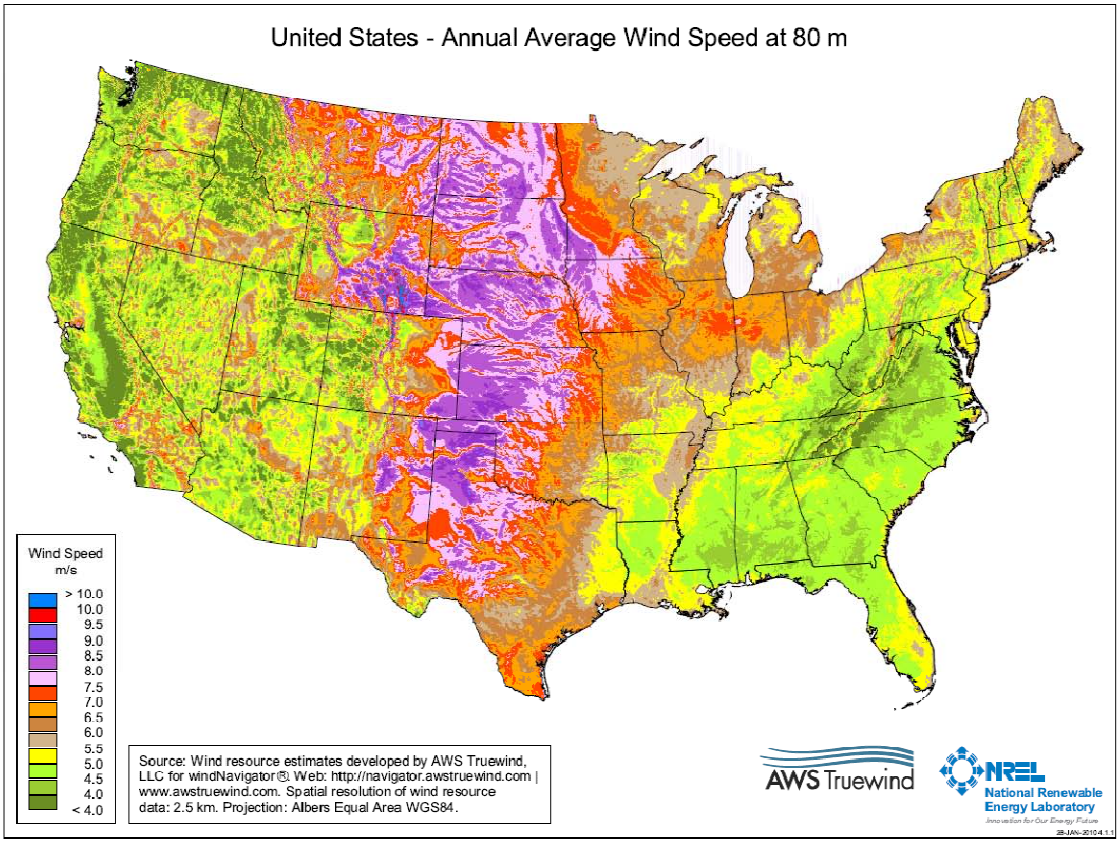

Figure 3: Wind map for United States [17]

1.2.2 Ground motion

The reason why structural engineers are focusing on dynamic loading is because in United States alone there are over a 1000 earthquakes each year that damage the infrastructure, including bridges, buildings, and traffic signs. Earthquakes are caused by the movement of plate tectonics. In United States there are three major fault zones where the earthquakes are more likely to occur.

In addition to earthquakes, ground motion can be caused by the vibrations transferred from the moving vehicles. This type of motion is more likely to take place on bridges. For that reason it is going to have an impact on the bridge sign structures.

1.3 Failure Mechanisms

1.3.1 Bending

Bending is one of the three leading causes of failure in highway signs. Failure in bending takes place when the applied forces tend to push the structure constantly in a certain direction and generate bending stresses that exceed the yield strength of the material. In utility poles bending stresses are introduced by the ground motion and wind loading. This is why the AASHTO Support Specifications for highway signs, luminaries and traffic signals requires that the wind and earthquake maps be updated regularly because they are both site specific. Changes in the loading criteria's can have a significant impact on the design of the structure, often leading in the reduction of material used which can save a considerate amount of resources. [8]

The simplest method that can be used to increase the yield strength is to either change the material type or sign dimensions, which would increase the cost in both cases. Most commonly, these structures are constructed from steel or wood. These days' composite materials such as fiber reinforced plastics (FRPs), due to their high strength, are being incorporated into the design. [1] However, using FRPs is considerately more expensive than using mild steel.

1.3.2 Shear

In addition to failing in bending, utility poles can fail in shear, similar to the way that buildings fail under earthquakes. These failures typically take place at the bottom of the poles, usually really close to the connection point to the ground. This happens due to the common procedures of erecting the structures by connecting them to the ground via rigid connections. In this case, the structure moves with the ground without any relative motion. A simple defensive mechanism that can be introduced to minimize the effect that a dynamic load might have on a structure is the installation of a base isolation system. A base isolation system is a simple mechanism that is used to decouple the structure from the ground. The isolation systems usually respond as a sliding unit. This mechanism can be used both in new construction as well as with retrofitting of those buildings which sustained damage in the past. One example of a building that has been retrofitted using base isolation system is the Koto building in Japan. This was one of many structures that were damaged during the Kobe earthquake. This building has been retrofitted in 1997 by using 12 lead rubber bearings.

1.3.3 Fatigue

Most common failure mechanism in sign structures is fatigue. Fatigue can be described as a mechanical failure caused by the interaction of loading, time and environment. Ordinarily, structures loading are uniaxial, multiaxial, monotonic, steady or variable. Loading can be applied for 10 seconds (ex. hammer impact), or it can go on for years (ex. bridges). Temperature and corrosion are some of the environmental effects that can impact the ability of the structure to handle the applied stresses. Interaction of these three, in addition to material properties, is what generates failure modes. [20] Fatigue failures occur in many different structures such as vehicles, ships, bridges, sign supporting structures and others. Fatigue can be classified as either low-cycle fatigue or high-cycle fatigue. The classification system is based on the period and amplitude of

vibration, as well as time to failure. [1] High-cycle fatigue takes place when the structure is subjected to loads that are significantly lower that the yield strain. Typically, over a million cycles is required to initiate high-cycle fatigue. Because of the nature of the loads, mainly wind, sign supporting structures generally experience high-cycle fatigue. Low-cycle fatigue takes place when the structure is subjected to strains that are larger than the yield strain. [5] The number of cycles required to initiate low cycle fatigue is rather small, sometimes just 10 cycles are enough to start crack nucleation.

Fatigue failure is common in structures that experience cyclic loading. For a light pole structures on bridges that type of loading is created by gusts of wind (Figure 4). Cyclic loading can, after a certain period of time, initiate crack nucleation in the foundation of the structure, which for bridges is almost always concrete. Once cracks are present, any loading can cause their propagation. For a bridge like Golden Gate in San Francisco (Figure 5), which supports hundreds of sign structures, detecting and fixing these types of cracks can be very expensive.

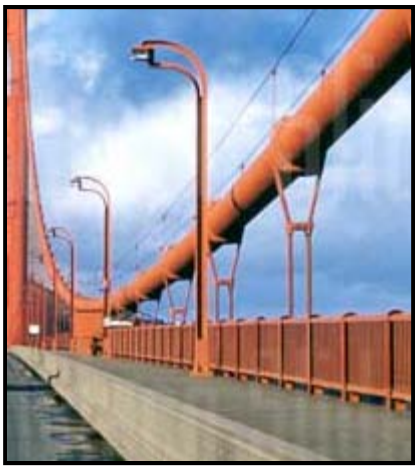

Figure 4: Light structure on Golden Gate Bridge in San Francisco [7]

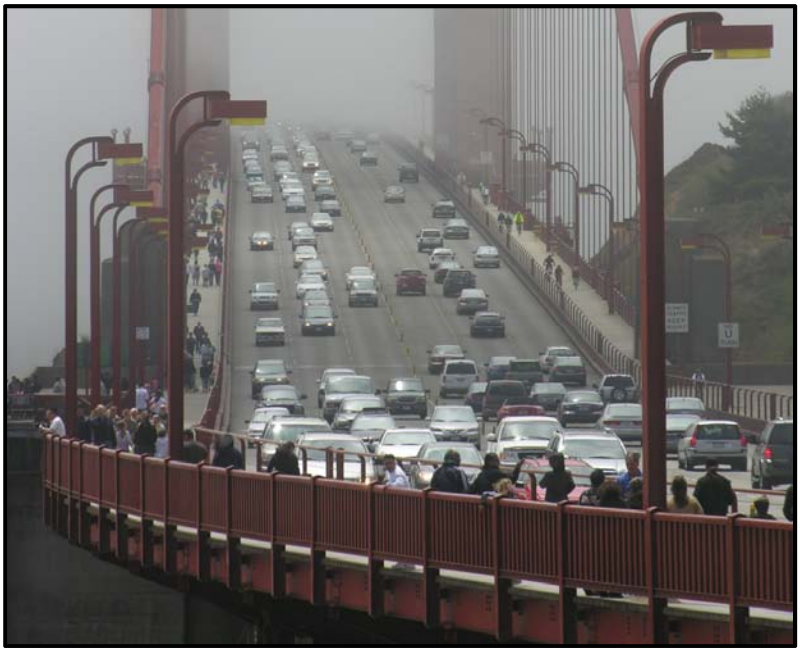

Figure 5: Light poles on the Golden Gate bridge (San Francisco) [21]

Recently, Departments of Transportation (DOTs) have indicated that there is higher concern for fatigue failure in signs carrying structures. Fatigue failure is caused by both the vibrations from the ground motion, as well as the natural wind loads. To extend the life of the structure AASHTO recommends that specific attention be applied to the connections, as well as any welding if it is used while creating those connections. [3] For the sign structures there are four types of loadings that cause fatigue damage, including galloping, vortex shedding, natural wind gusts and truck induced gusts. [8] Table 1 demonstrates the susceptibility for different support structures to these fatigues inducing factors. As can be seen all of the structures are susceptible to at least two factors. When the structure is susceptible to the loading it is marked with an X. For the bridge support structures, such as sign signal, vortex shedding has occurred in monotone bridge supports and cantilevered structures when the signal wasn't fully attached during installation. For the possible occurrence of vortex shedding in these structures that field was marked with a *. [6]

Galloping takes place on cantilever type structures which are constructed from several members. Consequences of galloping include generally large amplitude oscillations in plane perpendicular to the direction of wind. Even though cantilever sign structures consist of two members, galloping effects will only be evident on the arm.

Vortex shedding takes place when vortices of air shed around the pole. In that case changes of pressure are created from one side of the pole to the other. For the case when the natural frequency of the vortices matches that of the natural frequency of the sign resonance vibrations will take place.

Natural wind is a result of the wind forces around the structures. It is the basic and most common load that sign structures everywhere experience. It is very geography dependant (Figure 3).

Truck gusts are loads induced by passing vehicles. These wind loads apply both horizontal and vertical pressure on the structure. In this case critical stresses will be present on the vertically placed members.

Table 1: Fatigue loading factors [6]

Type of structure	Galloping	Vortex Shedding	Natural wind	Truck Gusts
Bridge support (Sign or signal)		*	X	X
Cantilevered sign	X		X	X
Luminaries		X	X	
Cantilevered Sign (one or two-chord)	X		X	X
Cantilevered sign (four-chord)			X	X

1.4 Guidelines and Implemented solutions

Past inspections of simple sign structures, cantilever structures and bridge supported structures have identified several critical issues that can impact their life expectancy. The problems observed were loose nuts and missing connectors on anchor and structural bolts, cracked anchor bolts, poor fit of flanged connections with cracked and missing bolts, cracked and broken welds, internal corrosion of tubular members and structural overload due to installation of signs that exceeded design square footage. [7]

Dampers can be used in order to regulate and lessen the response of the system to the loading forces. Applied control can be active, passive or semi-active. Active control is implemented by using active dampers, whose parameters can be changed to respond to varying loading conditions. Because they require large power sources they are the most expensive preventative measure. Passive control is accomplished with passive dampers, which are generally permanently attached to the structure. They are effective because they are capable of absorbing the energy that the system experiences upon loading. Semi-active control is implemented with hybrid dampers. Hybrid damper is a combination of the passive and active damper.

More frequent failure of sign structures due to fatigue and excessive vibrations started to be observed in the early 90's. In 1994 American Association of Highway and Transportation Officials (AASHTO) issued a report on the guidelines for sign support structures, known as the AASHTO *Standard Specifications for Structural Supports for Highway Signs, Luminaries and Traffic Signals*. [2] However, with more experience and knowledge, this report was proven to be incomplete. First changes to the report were implemented by the National Cooperative Highway Research Program (NCHRP). Four years after the original report NCHRP issued Report 412 which made the appropriate changed to the AASHTO's report. In 2002 NCHRP issued Report 469: *Fatigue-Resistant Design of Cantilevered Signal, Sign, and Light Supports*. In this study civil engineers focused on the fatigue failures and preventive measures in cantilevered structures. Three

main methods that can be applied to alleviate fatigue and vibration in cantilevered structures were identified. They include increase in stiffness, change in aerodynamic characteristics, and implementation of mechanical devices. Increase in stiffness can be accomplished by increasing dimensions of the structure or by changing structural configuration. This method prevents onset of galloping, and is the most expensive method that can be applied. Aerodynamic characteristics can be changed by adding damping plates and louvered backplates. Mechanical devices can be used to dampen the motion by reducing the intensity of oscillations. The idea behind all three of these was to improve mechanical damping in cantilevered structures. NCHRP's report focused on four research studies on cantilever structures including the study at University of Florida, Wyoming, Florida (Clearwater) and Texas Tech. [10]

University of Florida conducted several tests on a cantilever structure with a semituned impact damper. The damper consisted of a 3 ft long pipe, with inner diameter of 6-in, with a taper at the bottom. 15-lb ball was suspended inside the pipe with a spring. In order to allow the ball to move, its diameter was 2 inches smaller than that of the housing structure. This damper became known as the Florida damper. The tests performed on the structure included the free vibration tests, natural conditions tests as well as force vibrations with sinusoidal loading. In these entire tests damper performed well, lowering the horizontal displacement when the structure was mitigated and increasing the damping ratios. Laboratory experiments reported better results than those in the field. [10]

Wyoming Department of Transportation (WDOT) conducted several tests to determine the effectiveness of several different vibration dampers in improving mechanical damping. Their test subject was a simple cantilever structure (Figure 6).

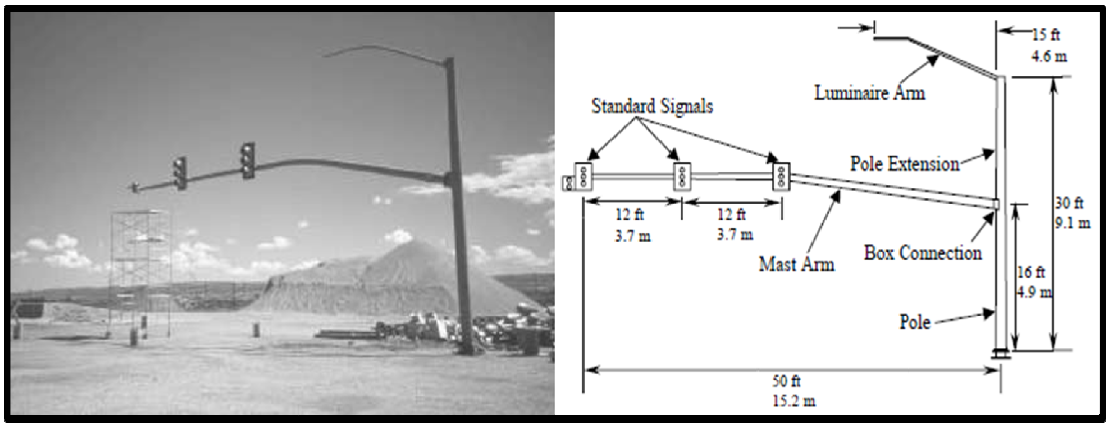

Figure 6: Cantilever testing structure

Tested dampers include in-plane strut damper, dual-strut damper, shot-put damper, Florida's damper, strand impact damper and elastomeric pad. By varying these devices and the fixing locations 15 different testing configurations were set up. Loading was applied with a mass oscillator, which varied the oscillations within 10 percent of the structures natural frequency. Half-power method was used to determine the damping ratios. While performing the experiments, researchers looked for an increase in the damping ratio for the mitigated structures for both in-plane and out-of-plane responses. In-plane motion is defined by the vertical motion of the arm (Figure 8), while the out-of plane motion is defined by the horizontal motion of the arm, as well as the swaying of the pole. An increase in damping ratio automatically proves that the moment is reduced.

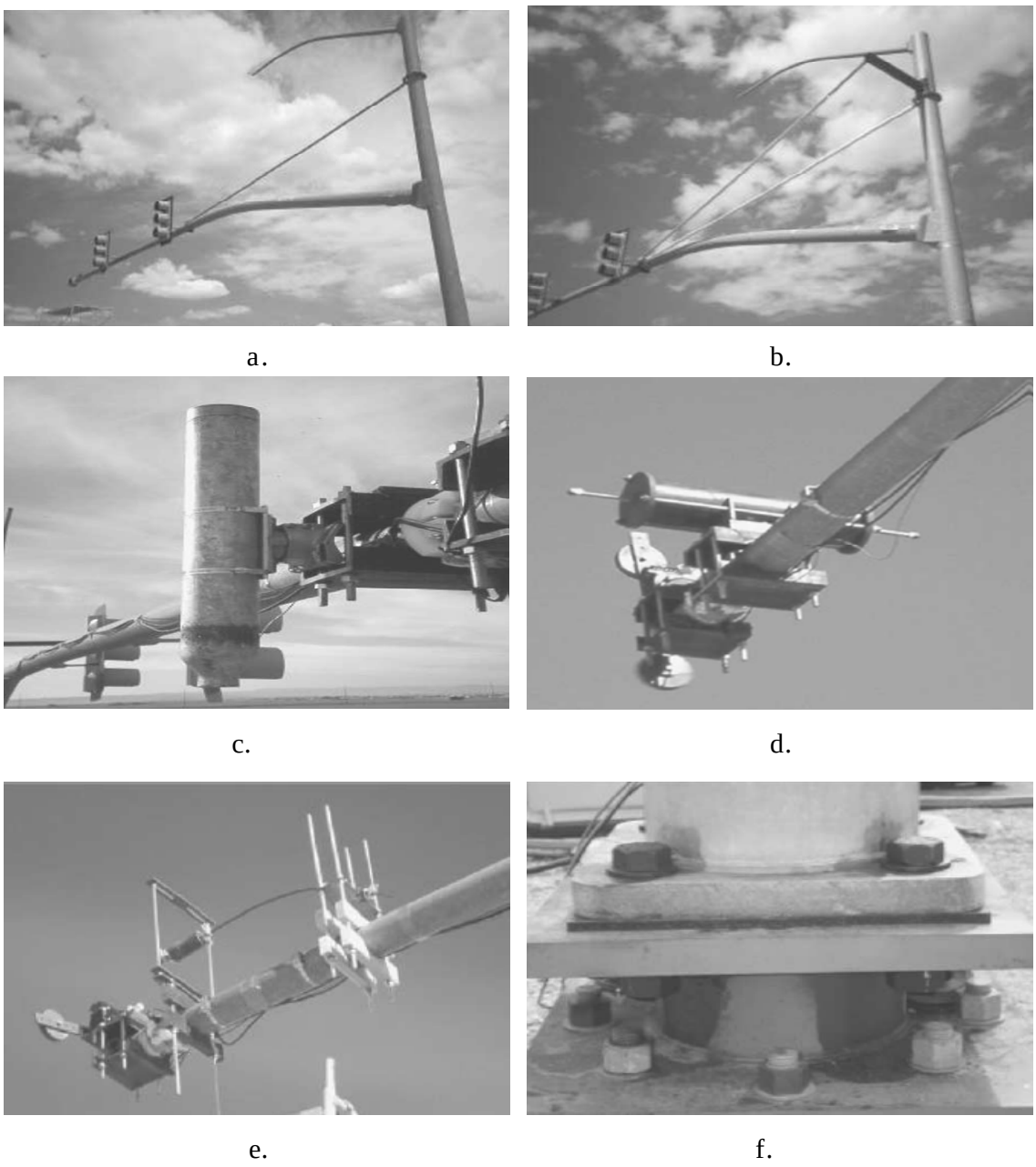

a. b.

c. d.

e. f.

Figure 7: Wyoming dampers (a. in-plane strut, b. dual-strut, c. Florida's damper. d. shot-put, e. strand impact, f. elastomeric pad)

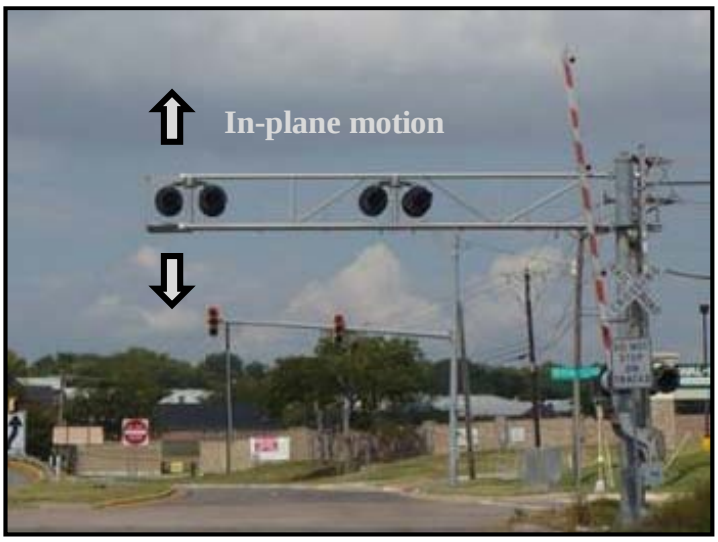

Figure 8: In-plane motion direction [4]

The first tested damper was the in-plane strut damper. This damper consisted of a 24-ft tube connected with the automobile shock absorber. In-plane strut damper linked the mast arm with the luminary extension. Results showed that in-plane strut damper was effective in increasing the damping ratio for the in-plane, while almost no difference was noted for the out-of-plane results. For the case where a dual-strut damper was used improvements were noted for both planes. Main issue with using strut dampers is that they require welding, and aren't always the most aesthetically pleasing. [10]

Another damper that was effective in increasing the damping ratio was the shot-put damper (Figure 9). Shot-put damper was attached at the end of the arm. Its effectiveness comes as a result of a ball moving inside the tube to counteract against any motion that the structure is experiencing from external loads. Some concern with using this device arises because of its heavy weight, approximately 100 pounds, as well as impact noise created by the shot-put rolling. [10]

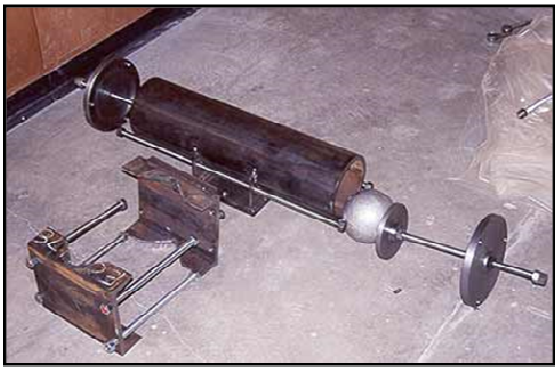

Figure 9: Shot-put damper

WDOT also tested Florida's semituned-mass impact damper, which also reported satisfactory results. Its biggest fault was impact noise. Strand impact damper was almost equally effective for in-plane and out-of-plane directions, making it an ideal damper for locations where considerable amount of force is applied in the out-of-plane direction. Out-of-plane loading is most often due to natural wind. Because the strand damper seemed to be the most effective it became known as the Wyoming-damper. As was the case with the shot-put and Florida's damper, strand damper also reported impact noises. In addition to testing dampers on the arm of the structure, WDOT also tested the effectiveness of elastomeric pad located under the baseplate. Elastomeric pad was able to increase the damping ratio. However, it also allowed motion of the baseplate relative to the anchor rods, making fatigue failure probable over a longer period of time. The last test conducted used both in-plane strut and elastomeric pad at the same time. Researchers wanted to see how two mechanisms, which both reported successes in orthogonal directions, performed together. Once again positive results were achieved for both in-plane and an out-of-plane direction, but the issue of relative motion was not eliminated. [10]

In 1999 researchers in Tampa, Florida wanted to complete several tests on a cantilevered traffic signal which was reporting severe vibration oscillations. Cantilevered

traffic signal was constructed by joining the mast arm to the post, using the standard built-up box connection. The original idea was to install strain gauges and damping devices, furthermore testing their effectiveness in mitigating vibrations under normal wind conditions. However, due to poor wind conditions they opted to use an alternative method, pull-down test. To complete a pull-down test rope was first attached near the tip of the mass arm, upon which tension forces were applied (Figure 10). Once it was believed that the structure was sufficiently excited the rope was released, and free vibration response was recorded. [10]

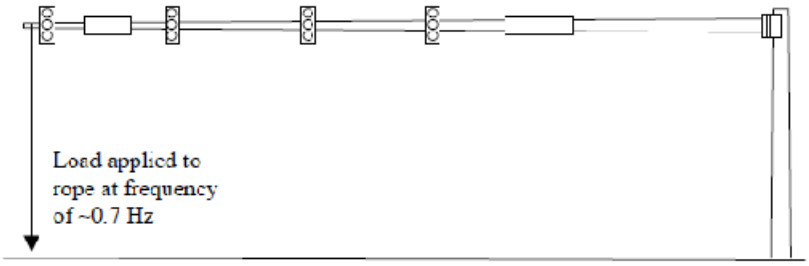

Figure 10: Cantilever signal structure (Florida's pull-down test)

Eight strain gauges were installed on the structure, four on the mast arm and four on the post. In addition, accelerometers were placed near the mast arm tip. Datalogger was used to read the strain results. Nine different tests were performed, where the initial vertical displacement was varied. The tests showed that the magnitude of the

displacement had little effect on the calculated damping ratios of the structure, both for unmitigated and mitigated cases. Three different damping devices were used for this structure including early prototype of the Florida impact damper, damper used on transmission towers, and Wyoming's strand damper. Florida impact damper consisted of a steel cylinder with and enclosed mass hanging from a spring which once in place acted as a semituned mass damper. The transmission tower damper was made of a polyvinyl chloride tube which was partially filled with sand. The device was unsuccessful in increasing the in-plane damping ratio because the movement of the arm wasn't enough to move the sand within the tube. This damper did report small increases in the out-of-plane damping ratio. Wyoming's stand damper initially acted as an impact damper but changed into a semi-tuned mass damper after a few initial cycles. It reported increases in the damping ratios for both planes. Table 2 shows the summary of the Tampa testing. [9]

Table 2: Tampa cantilevered structure results

Mitigation device installed	Average In-Plane Frequency (Hz)	Average In-Plane Damping Ratio	Average Out-of-Plane Frequency (Hz)	Average Out-of-Plane Damping Ratio
None	0.668	0.13 %	0.615	0.57 %
Florida Impact Damper	0.619	0.76 %	0.581	0.54 %
PVC-Sand damper	0.658	0.13 %	0.608	0.66 %
Wyoming Strand Damper	0.630	0.54 %	0.585	1.14 %

The forth damper, known as “snubber” damper (Figure 11), was initially planned to be tested on the Tampa’s cantilever sign structure but was instead tested at the University of Florida. In the damper design 3/16–in steel cables, 5 ft in length, was attached to the corners of the mast arm and column. This set-up was designed for the pull-down tests. However, the experiments proved that the damper performed poorly when large initial displacements were applied. Consequently, this type of device could only be used for structures where small initial displacement is expected. [9]

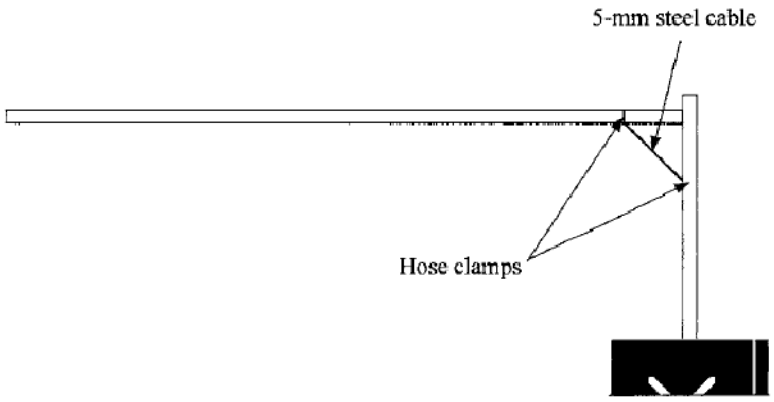

Figure 11: Snubber damper [9]

In 1999 Texas Department of Transportation (TDOT) supported several experiments where galloping mitigation was studied on cantilever sign structure. The tests were performed by Texas Tech University. Four years prior Texas Tech did another study on the favorable conditions for galloping. [9]

For the tests cantilevered sign structure was constructed on a rotatable base. This was necessary to ensure that the winds would impact the structure behind the mast arms, creating favorable conditions for galloping. To begin with, four strain gauges were installed on the post. Tests were performed under wind speeds ranging from 4 – 16 mph. They proved that the NCHRP Report 412 was accurate in recommending galloping load of 21 psf. By reason of unfavorable wind conditions for galloping only one mitigated test was performed, instead of the planned five. That test was performed using Wyoming's strand damper. These tests confirmed that using Wyoming's strand damper will significantly increase in-plane damping ratio of the structure. In addition, over a period of five days, 24 galloping tests were performed, first 16 lasting 5 minutes while the remaining 8 were extended to 20 minutes. The results show that the unrestrained damper reported smaller in-plane stress ranges meaning that using unrestrained damper can reduce the impact of galloping near the column base. [9]

1.5 Project Objective

The objective of this project was to analyze the effectiveness of a damper in extending the life of a highway sign structure. Low cost passive damper was designed and tested in the lab. Structure was subjected to pull test, meant to simulate gusts of wind, as well as ground motion by use of a shake table. Data was collected using accelerometers and strain gauges. Fatigue, bending and shear are the leading causes of failure in these structures. For that reason, damper's effectiveness was evaluated by its capability to lower the effects of fatigue, bending and shear forces.

CHAPTER II
THEORETICAL BACKGROUND

2.1 Vibrations background

Vibration refers to the repeated motion of the rigid and deformable systems. Depending on its magnitude, vibration can cause significant amount of damage such as those involve during seismic and high wind activates. With small magnitude, vibration can cause unwanted motion to the structure that may induce a fatigue type failure with time. Therefore, there have been significant amount of work to design systems to mitigate the effect of vibration on the structures. One major field is the design of vibration suppression systems.

2.1.1. Vibration suppression

Vibration suppression reduces the shake severity and damage occurring to the structures caused by strong winds, earthquakes, and traffic by using mechanical devices such as dampers. The vibration suppression can be done using vibration control systems based on active, passive or hybrid systems. Vibration control is the design or modification of a system to mitigate unwanted vibrations or to reduce force or motion transmission. This can be done by changing the inertia, stiffness, damping, and even the configuration of the system.

One example of vibration isolation is to attach a vibrating mass to the floor using a spring and a damper as shown in Figure 12. The transmitted forces to the ground due to this type of arrangement can be determined using Equation 1.

$$F_T = kx + c\dot{x} \qquad \text{Equation 1}$$

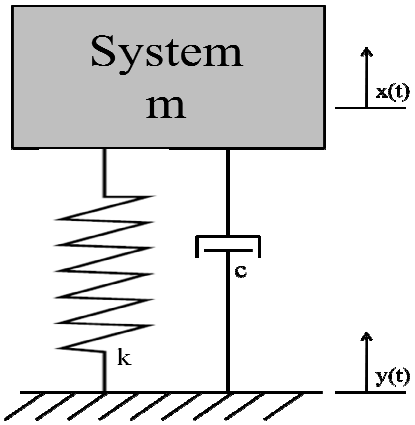

Figure 12: Mass damper system

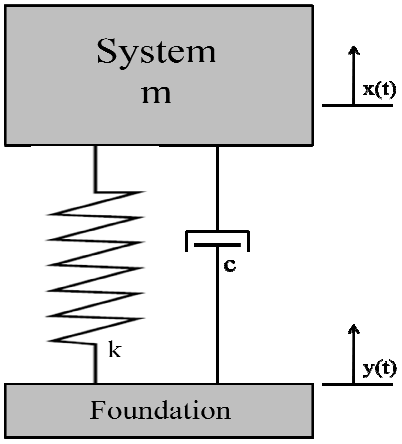

Figure 13: Isolated mass damper system

On the other hand, if the foundation is allowed to move relative to the vibrating mass as shown in Figure 13, then in this case the force transmitted to the foundation would be related to the relative motion between the foundation and the vibrating mass z (t), where z(t) is the difference between x(t) and y(t).

$$\ddot{y} = -\frac{\left(kz + c\dot{z}\right)}{m} \qquad \text{Equation 2}$$

A spring-mass system can be used to simplify the analysis of complicated systems for the purpose of having some insight into the characteristics of the system motion. For more detailed analysis, advanced numerical schemes such as commercial finite element software are used. Figure 14a depicts a schematic drawing of a single-degree of freedom spring-mass system. The equation of motion for this system can be seen in Equation 3. In the cases where a material with a high damping coefficient is used damping coefficient has to be incorporated into the equations of motion (Figure 14b). Equation 4 illustrates the equation of motion that describes this system. In this case the natural frequency can be calculated by simply taking the square root of the stiffness and the mass of the structure (Equation 5).

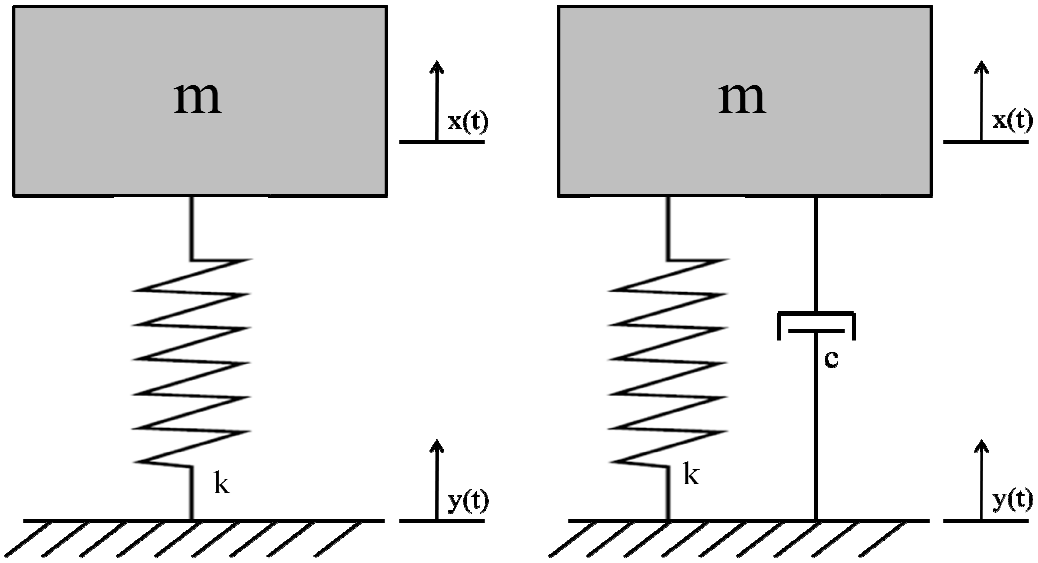

a. b.

Figure 14: Mass Damper
(a. no damping, b. damping)

$$m\ddot{y}(t)+ky(t)=f(t) \qquad \text{Equation 3}$$

$$m\dot{y}(t)+c\dot{y}(t)+ky(t)=f(t) \qquad \text{Equation 4}$$

$$\omega=\sqrt{\frac{k}{m}} \qquad \text{Equation 5}$$

The highway signs are normally constructed from tubular beam, column like elements (Figure 15). The stiffness of such structural units can be estimated using analytical beam analysis. Before the analysis can be completed it is necessary to identify all of the material properties (Table 3), dimensional parameters (Table 4) and other parameters such as the area, volume and weight of the structure (Table 5).

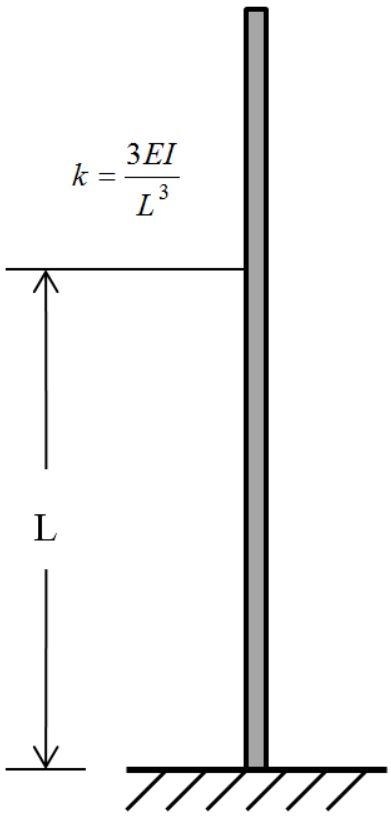

Figure 15: Beam analysis

Table 3: Material properties for steel

Material properties for steel	Value
Modulus of Elasticity - E	$29x10^3$ ksi
Poisson ratio - ν	0.3
Density - ρ	0.284 lb/in^3

Table 4: Dimensional parameters of the pipe

Physical parameters	Length (in)
Outer diameter - d_o	1
Outer diameter - d_i	0.93
Length - L	37

Table 5: Calculated parameters of the pipe

Parameter	Value
Area - A	0.106 in^2
Volume - V	3.926 in^3
Weight - W	1.115 lb
Mass - m	0.035 slugs = 0.00289 lb s^2/in
Moment of Inertia - I	0.0124 in^4

By incorporating the values from the Tables 2-4, Figure 5 and Equation 5 it can be determined that the stiffness of the pipe is about 21.24 lb/in. Therefore the angular velocity of the pipe is about 85.85 rad/s, and the frequency is 13.66 Hz.

2.2 Transmissibility

Transmissibility of a system can be defined as ratio between the magnitudes of the input signal entering the system to the magnitude of the signal coming-out of the system. It measures how much of the input energy is transferring to system. For simple harmonic motion, such as sine signals, the transmissibility can be computer in the time domain using for example the ratio of the output acceleration to the input acceleration. [16]

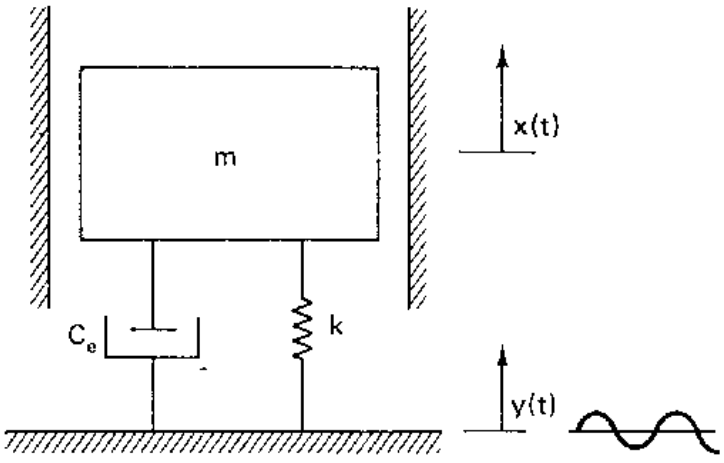

Figure 16: Mass damper system [5]

For a simple mass damper system (Figure 16) transmissibility can be calculated using Equation 6. [5] In order to fully understand the impact of the damping coefficient, ξ, transmissibility was plotted versus the ratio of the frequency and natural frequency. Such a plot for different values of ξ can be seen in Figure 17. If the frequency of the applied signal matches the natural frequency of the structure resonance will take place. On the transmissibility plot when the ratio of the two frequencies is one, resonance is taking place. By varying ξ the impact of damping on transmissibility and amplitude of frequency and vibrations during resonance can be illustrated. When there is no damping ($\xi = 0$) transmissibility curve has a very sharp peak, and as ξ value is increased the curve's sharp peak gets smoother and smoother.

$$T = \frac{\sqrt{1+\left[2\xi\left(\frac{\omega}{\omega_n}\right)\right]^2}}{\left[\sqrt{1-\left(\frac{\omega}{\omega_n}\right)^2}\right]^2+\left[2\xi\left(\frac{\omega}{\omega_n}\right)\right]^2} \qquad \text{Equation 6}$$

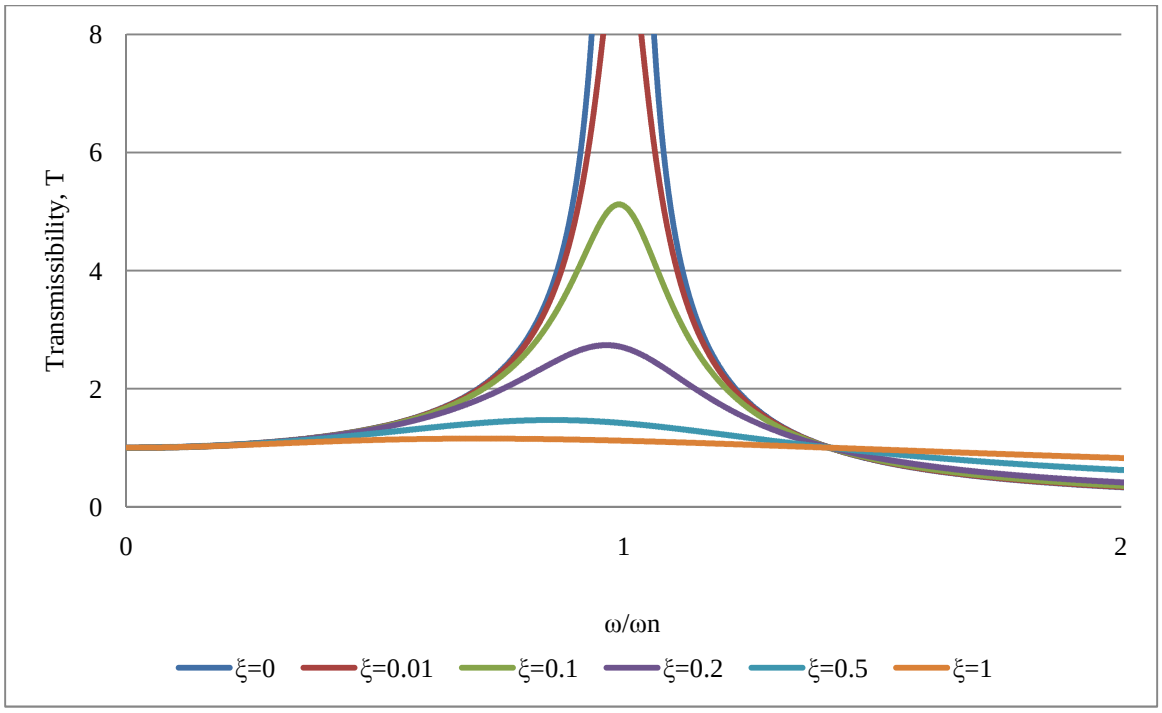

Figure 17: Transmissibility

While it is constructed from a one degree of freedom mass-spring system, still the transmissibility plot of Figure 17 contains very useful information that can be used to understand and assist in the designs and the behaviors of complex systems. For example, increasing the mass of the structure can lower the natural frequency and increasing its stiffness can increase the natural frequency. By adjusting the latter quantities and choosing appropriate damping, the designer can avoid resonance situations and to reduce the forces transmitted from the system to the foundation and vice-versa.

For random complex signals such those resulted from the seismic effect, traffic loading, and winds, the analysis should be done in the frequency domain using Fourier transform. The transmissibility in this case can be calculated as the ratio between the cross spectral density of the input and the output signals divided by the auto spectral density of the input as shown in Equation 7.

$$T(\omega) = S_{xy}(\omega) / S_{xx}(\omega) \qquad \text{Equation 6}$$

Where TR is the transmissibility, S_{xy} is the Cross Spectrum, and S_{xx} is the Auto Spectrum; subscripts x and y stand for the input and the output.

Cross spectra is computed by multiplying the Fourier Spectrum of a measured response by the complex conjugate of the Fourier Spectrum of the reference DOF. The result is a complex number that has both magnitude and phase, where the phase is the phase difference between the two measurement points. Cross spectrum can be calculated using Equation 8.

$$S_{xy}(\omega) = S_x(\omega) / S_y^*(\omega) \qquad \text{Equation 7}$$

Where $S_x(w)$ is the Fourier Spectrum of the measured response, and S^*_y is the Fourier Spectrum of the reference DOF. Auto spectrum can be determined using Equation 9.

$$S_{yy}(\omega) = S_y(\omega)\, S_y^*(\omega) \qquad \text{Equation 8}$$

In this work, the transmissibility will used as the measure of the effectiveness of the proposed dampers. In this case, the transmissibility of the input signal from the shaker will be correlated to the motion of selected points on the pipe. In order to determine transmissibility commercially available software was used. In this case transmissibility will also be referred to as operational deflection shape (ODS).

One of the greatest advantages in determining transmissibility is that it allows the user to see the deflection of the structure at any frequency, not just the natural frequencies. An example of an ODS curve can be seen in Figure 18. In this case, the deflection curve was plotted for a frequency of 36 Hz, which is not a natural frequency of the structure. If the selected frequency was a lot closer to the natural one resonance type of behavior would start to take place and animating these results would show an increase in the amplitude of the oscillations. ODS illustrates the true behavior of the structure under loading. In order to get smoother deflection curves the data should be collected for a larger number of points.

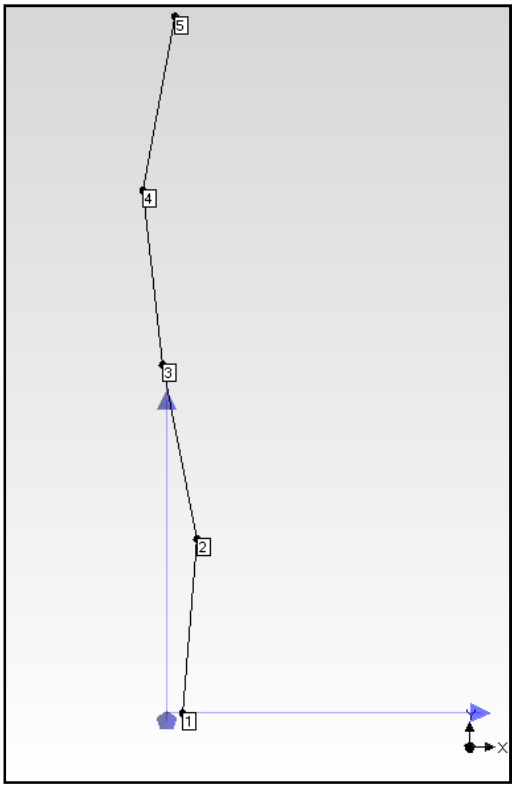

Figure 18: ODS for Kobe_EW [36 Hz]

2.3 Fast Fourier Transform (FFT)

In real life, sign structures are affected by gusts of wind, hurricanes, as well as ground motion that can be due to both vehicles passing by and earthquakes. In most of these cases the loading is not harmonic and boundary conditions are complicated, making the task of predicting modal frequencies very complex. One way of doing this is to perform a Fast Fourier Transform if the acceleration data is available.

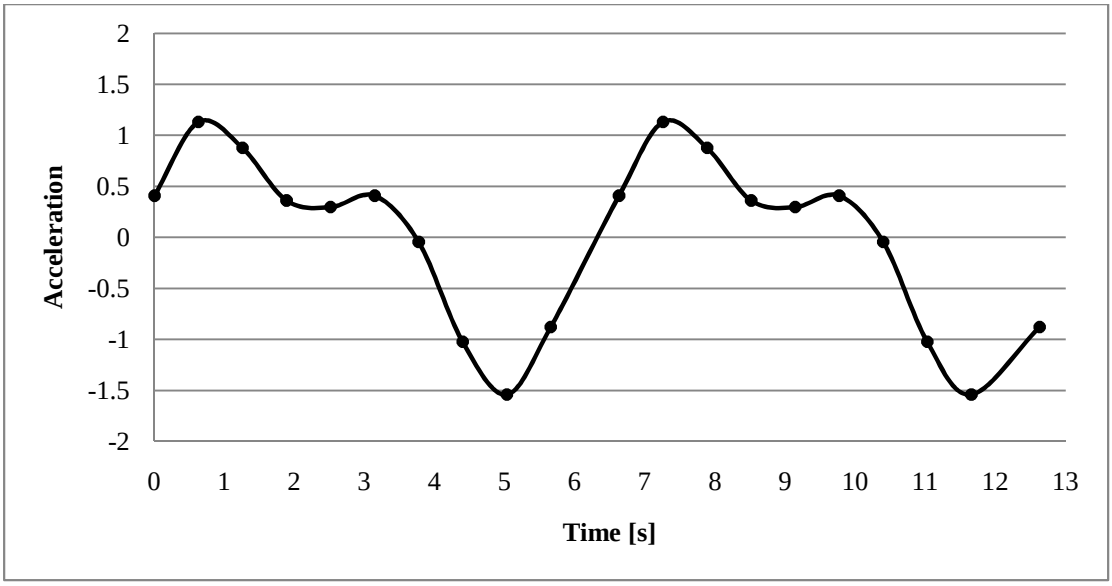

Figure 19: Random time signal

Figure 19 illustrates a section of what that type of loading could look like. In a case such as this there is periodicity which means that the acceleration signal replicates itself after a certain time period T (Figure 20).

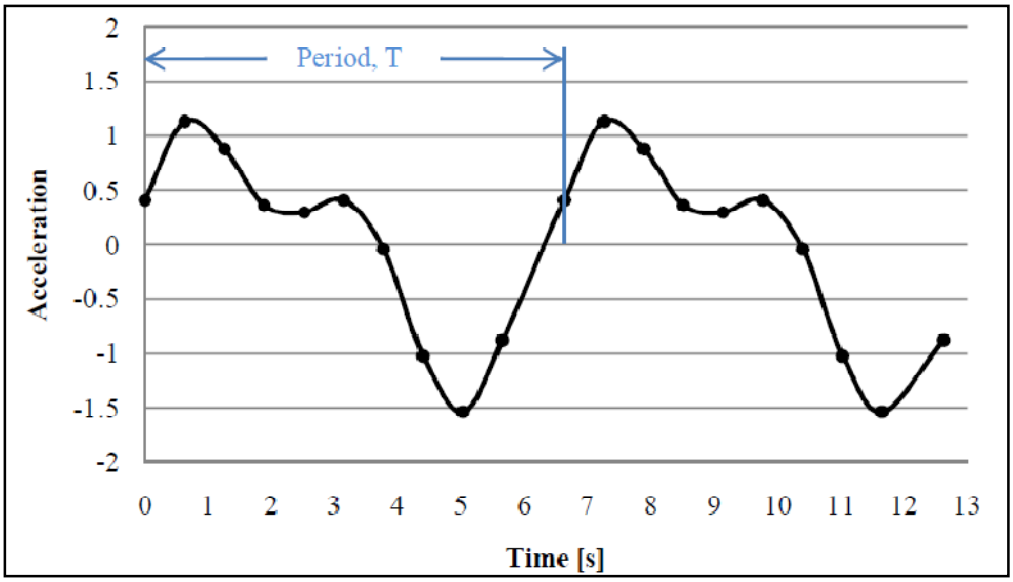

Figure 20: Periodic time signal

Discrete Fourier transform makes is possible to analyze the frequencies and amplitudes of such signals, with the end results simply being a graph of frequency versus amplitude. For the signal presented in Figure 19 the amplitude and frequencies can be seen in Figure 21.

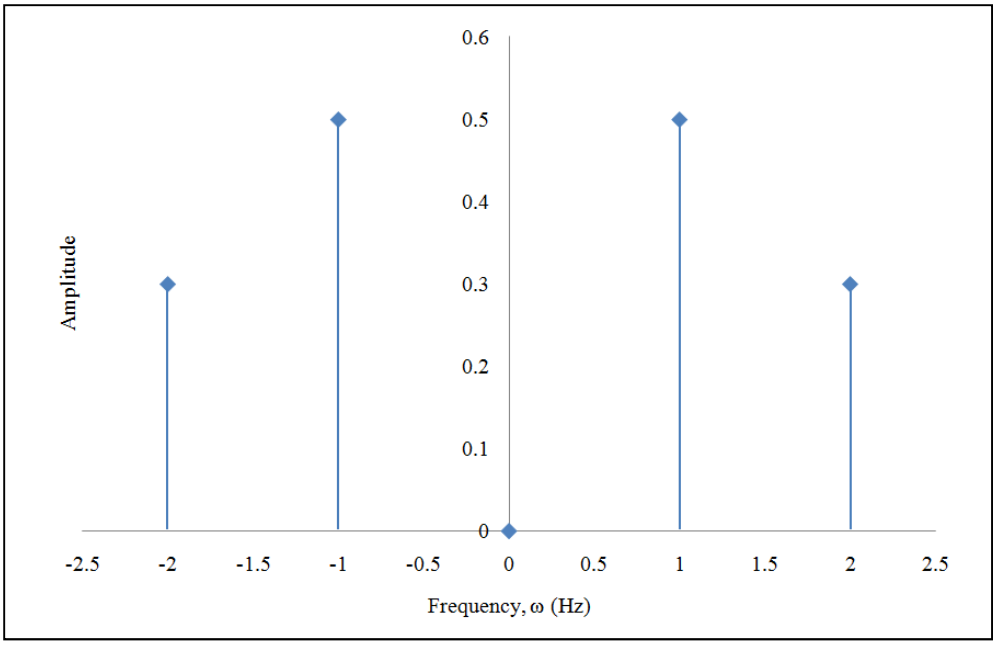

Figure 21: Frequency domain

The reason why such an analysis is important is because in the case where the loading frequencies equal the natural frequency of the structure resonance will take place. Fourier Transform is one of the most widely used methods to analyze the applied loads. Today there are many software packages available that have the Fourier Transform build in, such as Mathematica, Excel, Matlab and others. In many cases, such software works with data collecting system to make the analysis simpler.

2.4 Strain

Strain was used as another measure to quantify the effectiveness of the proposed damper. In this case, the strain on the outer surface of the pipe was measured experimentally using strain gauges. Assuming linear elastic behavior, the resulting strain will reflect the magnitude of the bending stresses generated in the pipe due to vibration. Strain was collected on the base point.

2.5 Horizontal Ground Motion

The last measure for the effectiveness of the proposed damper is based on the magnitude of acceleration of the base mass relative to the ground motion. This can be measured by the magnitude of the transmissibility occurring in the horizontal direction between the base mass and the ground. In this case it is a complex motion due to the involvement of the rubber pads in mitigating the energy and the contribution to the relative motion.

CHAPER III
ANALYTICAL ANALYSIS

3.1 Modal Analysis

Due to the complex form of the vibration involved in this work, most of the analysis will be conducted in the frequency domain. The modal parameters of the structure represented by the natural frequency, mode shapes, and modal damping will be the basis for the changes in the system response because of the addition of the damper. Modal analysis is traditionally used to calculate the modal parameters. In this case, the system can be simplified and analytical methods can be used to calculate the modal parameters. When the system becomes more complicated and in order to generate more reasonable results, numerical methods are used toward this end. One available option is to use commercially available software's such as ANSYS. ANSYS is finite element method software that has the capability to perform modal, harmonic, time transient and other dynamic analysis.

In the numerical modal analysis, the first step requires the selection of the elements. In this case Beam 3 – 189 elements were selected and used to create a mesh of 100 elements. Key-points were used to define the height of the structure to be 37 in. Pipe was selected as the common cross section, and modeled by specifying the outer radius of 0.5 in, and the inner radius of 0.465 in. The meshed model looks like the beam in Figure 6. Once mesh was created modal analysis was performed using the Block Lanczos method. Overall 100 modes were extracted and expanded.

In addition to the base pipe model, two other models were created, one with base mass and another with rubber. All three can be seen in Figure 22.

Figure 23shows the first five modes with their corresponding natural frequencies for the case where the pipe is modeled without the additional base-mass, while Figure 24 demonstrated the five mode shapes and their corresponding natural frequencies considering the base-mass in the modeling of the system.

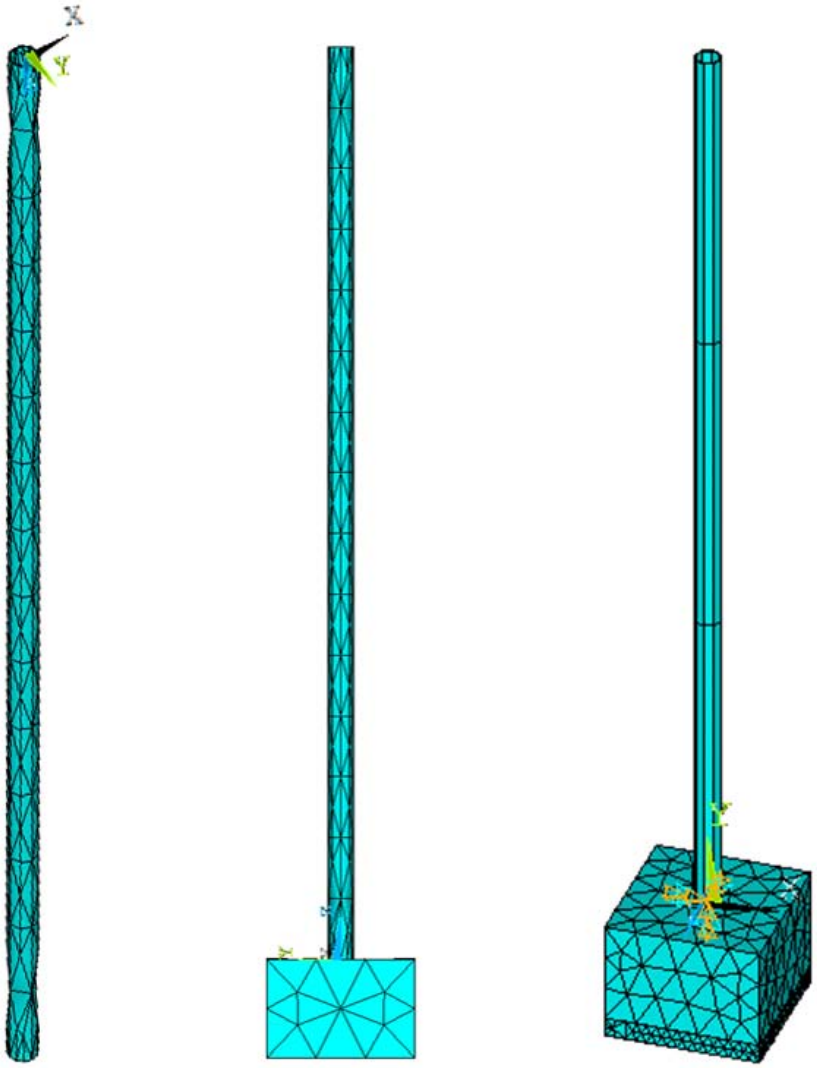

a. b. c.

Figure 22: ANSYS models
(a - pipe, b - mass, c - full damper)

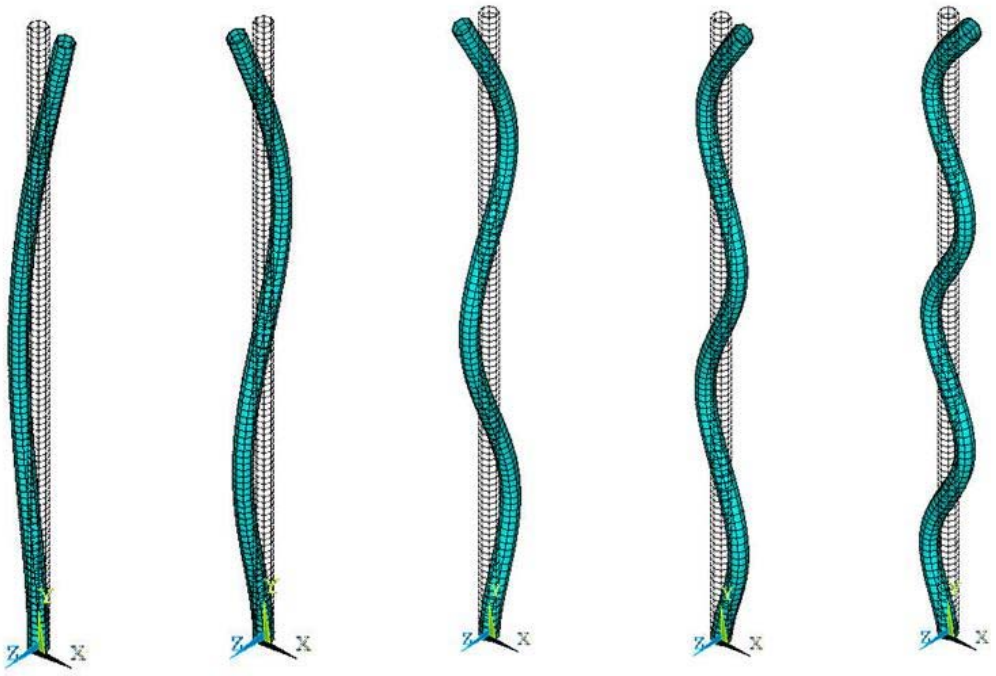

Figure 23: ANSYS first five modes

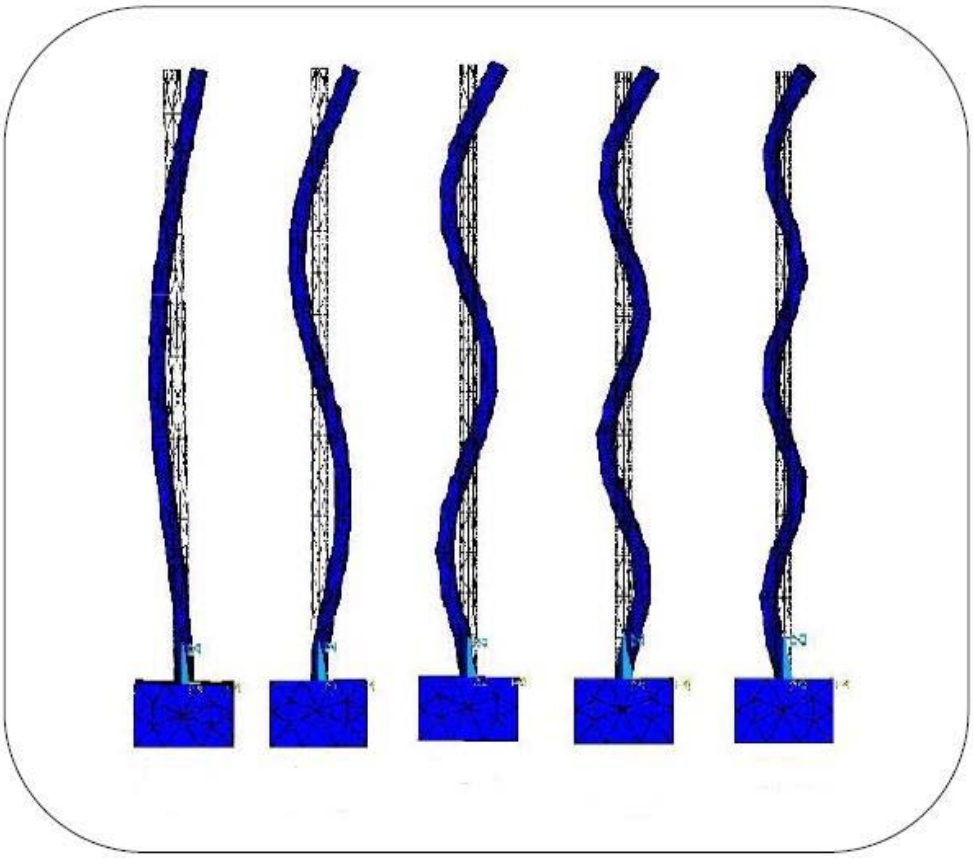

Figure 24: ANSYS model with mass (10 m)

Table 6 lists the first five mode shapes for all three systems.

Table 6: ANSYS Modal Analysis results

Mode of vibration	Frequency [Hz]		
	1-M	10-M	Fully damped system
First mode	8.76	9.27	9.38
Second mode	24.24	23.84	24.01
Third mode	46.7	45.89	45.80
Fourth mode	75.73	74.61	74.70
Fifth mode	110.51	109.7	109.142

CHAPTER IV
METHODS AND EXPERIMENTATIONS

4.1 Damper design

The proposed damper of this work was designed to mitigate the three main causes of the sign's failure. Particularly the shear forces at the base of the sign due to the horizontal motion, the bending stresses at the surface of the pipe due to bending caused by gusty winds, and the fatigue stress represented by the low cycle high amplitude vibration and the high-cycle low magnitude vibration.

The proposed damper is a passive system that consists of two components. A large mass (ten times the mass of the main pipe of the sign) attached to the base of the pipe and pads of visco-elastic materials (rubber) to isolate the base mass from the foundation. The intention of the added mass was not increase the degree of freedom of the system, but was to increase the mass of the sign and shift the natural frequency of the sign to the lower end. The base mass will also work as a restoring element and bring the sign to its vertical static position as quickly as possible minimizing by that the number of vibration cycles. The base mass, on the other hand, will magnify the magnitude of the shear force induced with the foundation. However, the addition of the rubber pads will work on generating a relative motion between the base and the ground and will work on dissipating the shear force energy through the shearing of the rubber pads.

The design process of the damper also considered the practicality of the propose system and the way it will be used in real-life scenarios. Thus, the damper was design considering the easiness in assembly and installation in the field. The step of installing the damper with the sign in the field will start by constructing a rectangular concrete hole. The next step involves inserting the rubber pads to the base and the walls of the hole. The sign with the rectangular base mass will be then inserted inside the runner housing. A cover plate will be used to hold the system to the ground. The proposed installation

method is very similar to the traditional normal practice procedures used without dampers.

4.2 Damper construction

A stop sign was selected in this work to represent a sample of a highway traffic sign. The shake table used was the only one available in the Civil and Environmental Lab. Due to limitations in the pay load capability of the shaker available for the testing; the size of the sign was scaled down using similitude analysis. The shaker table cannot support more than 100 lb of weight. Upon the completion of the dimensional similitude a cylinder with a height of 3.5 ft, diameter of 2 in and thickness of 0.065 in was selected to represent a standard highway-stop sign. This size was selected because it is commercially available and because it is exactly half the size of the normal sign. The cylinder was constructed from standardized steel and the elastic material properties can be seen in Table 3. Basic dimensions for the damper and the pipe can be seen in Figure 25. The cross section of the damper can be seen in Figure 26.

The second step in the construction of the model required the design of the damper. After looking into using rubber pads and composites, neoprene composite was selected as the damping material. These pads (Figure 27) are manufactured by Kellet Enterprises Inc., a proven manufacturer of vibration isolators' pads, and absorbing pads. This vibration absorber is the first three layer shake absorber patented in the United States.

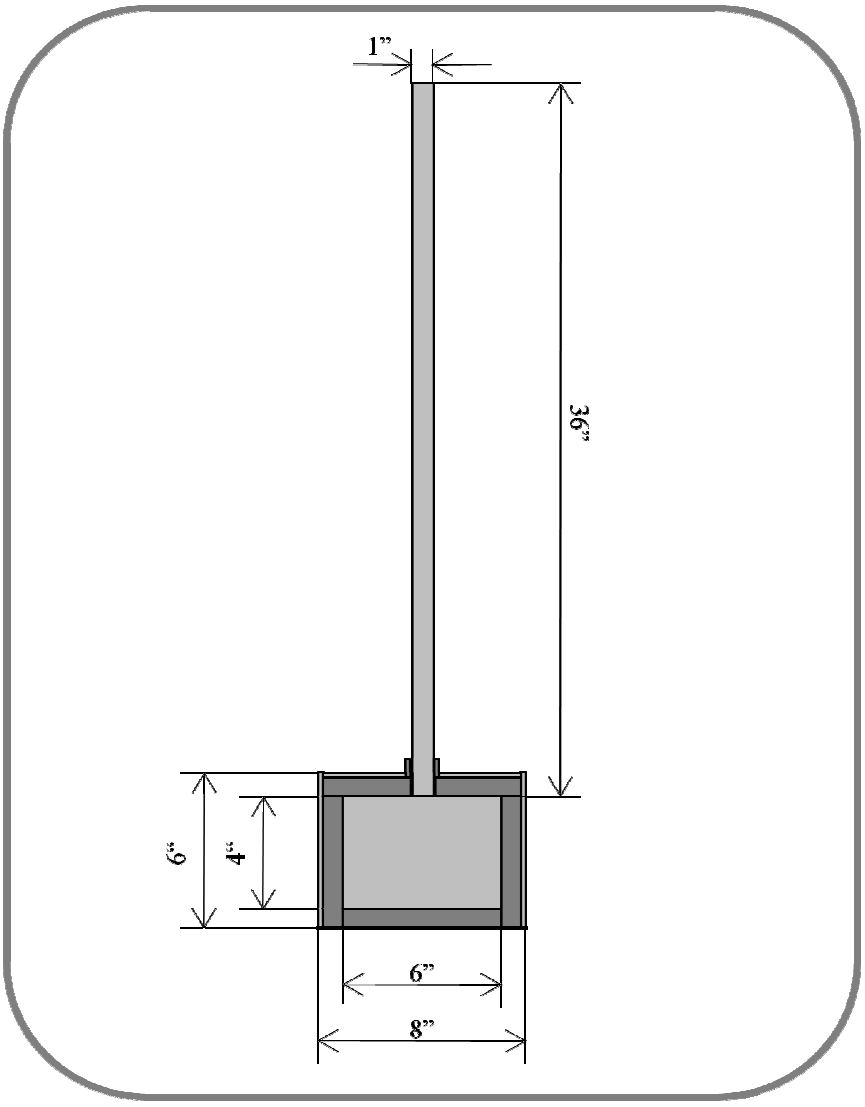

Figure 25: Model dimensions

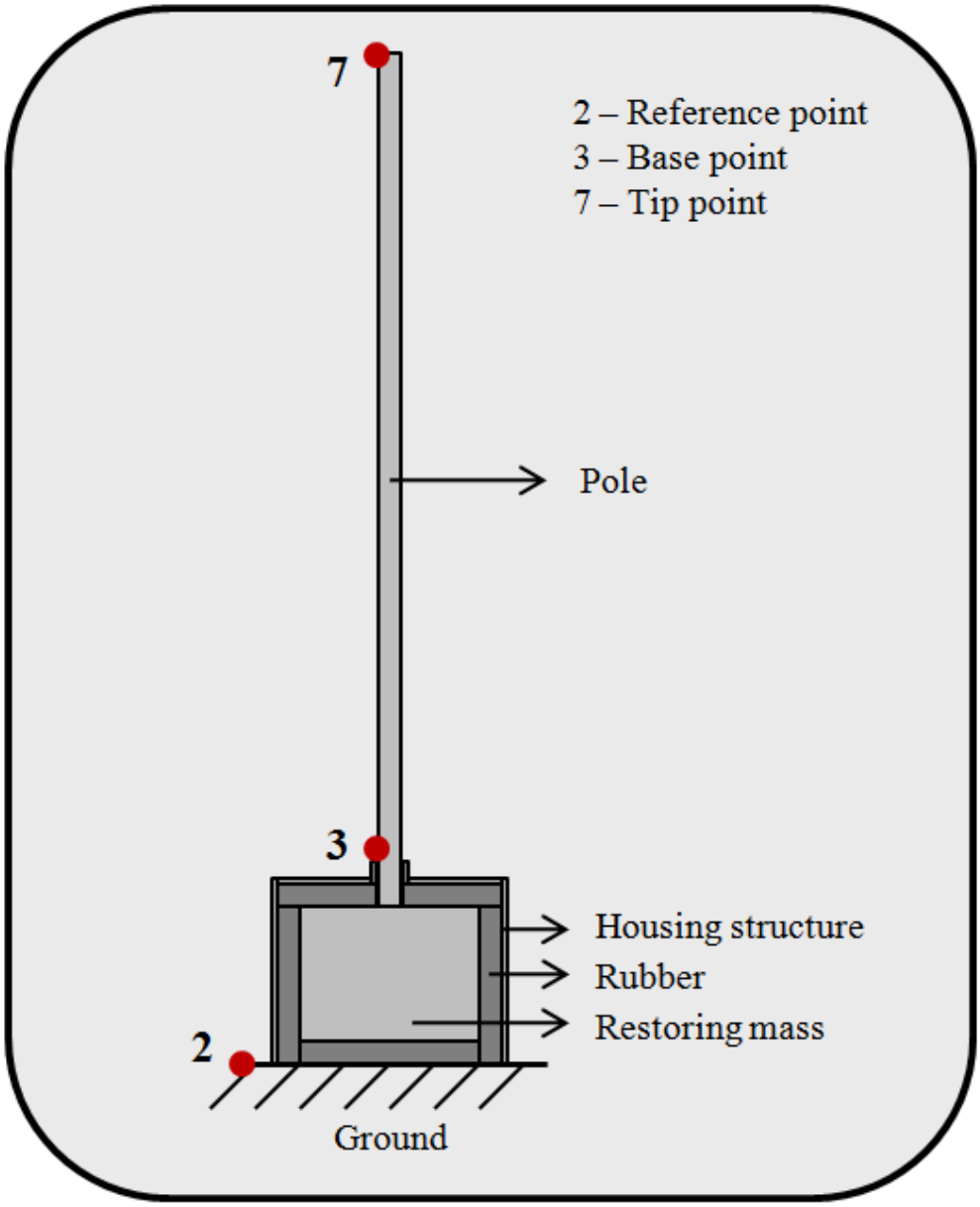

Figure 26: Sign

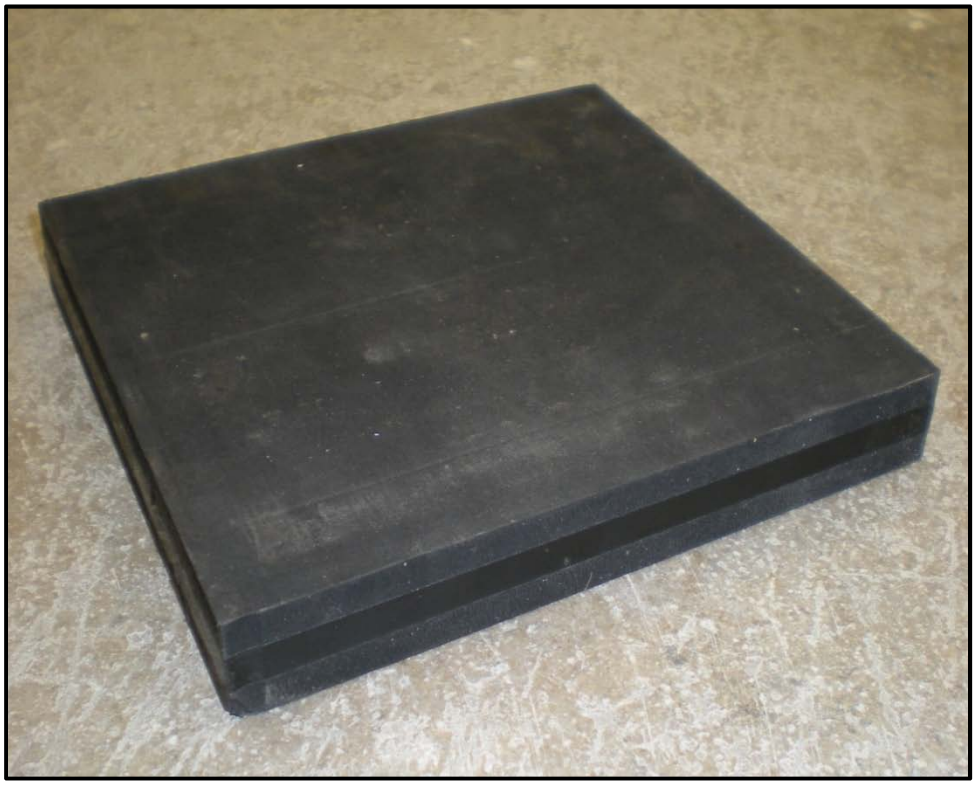

Figure 27: Rubber composite

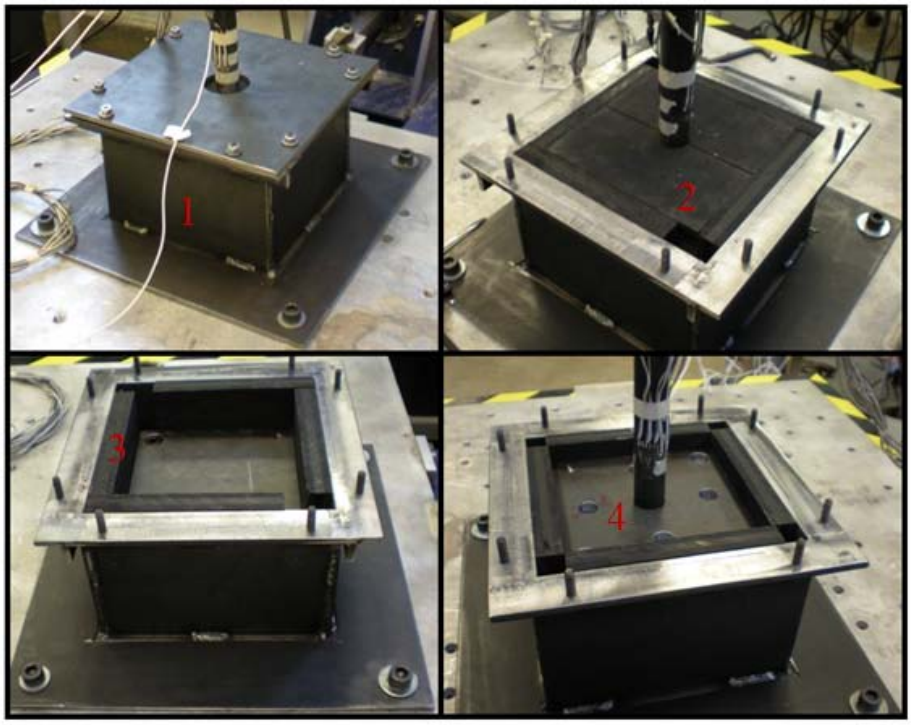

1. Housing structure with cover
2. Top rubber
3. Side rubbers
4. Restoring mass

Figure 28: Damper

The damper (Figure 28) was manufactured at the Engineering Shop at the University of Iowa. The outside box was welded together using steel plates with the thickness of a ¼-in. Once the box was created it was then welded to the bottom plate that allowed the model to be screwed onto the shaker table. For the inside of the box the damping pads were cut into specific sizes in order to completely surround the weights in the middle of the damper. There were four different weights which were simple steel plates with a thickness of 1-in. All of them were bolted together which allowed for easy disassembly. The fourth weight had the pipe attached to it. In addition, it had the holes which allowed it to be attached to the shaker on its own. This way testing could be done for the pipe without the damper and the results could be compared.

4.3 Damper testing

In order to evaluate the quality and effectiveness of the damper, the system including the pipe and the damper were attached to the shaker table, where the system was tested under the effect of several external random excitations. Two types of excitations were used. The first type was by using mitigated earthquake signals to represent ground motion due to traffic and possibility earthquake. The second type of excitation was performed by pulling the free end of the pipe to a certain level and then let it freely vibrate. The second type of loading was used to simulate the effect due to natural and wind traffic gusting.

Experimental modal analysis was used to analyze the response of the system by using the concept of operating deflection shape (ODS) to find the ratio between the input signals and several selected output points on the structure. In this work ODS represents transmissibility. Six accelerometers were used in the experiments, one was attached to the shaker table base and five were attached to points on the pipe to measure the accelerations (Figure 29). Additional ODS analysis was performed using only two accelerometers, one at attached at the shake table and another on the base point (Figure

29). Two single direction strain gauges were attached to the outer surface of the pipe closer to its base where it meets the base-mass.

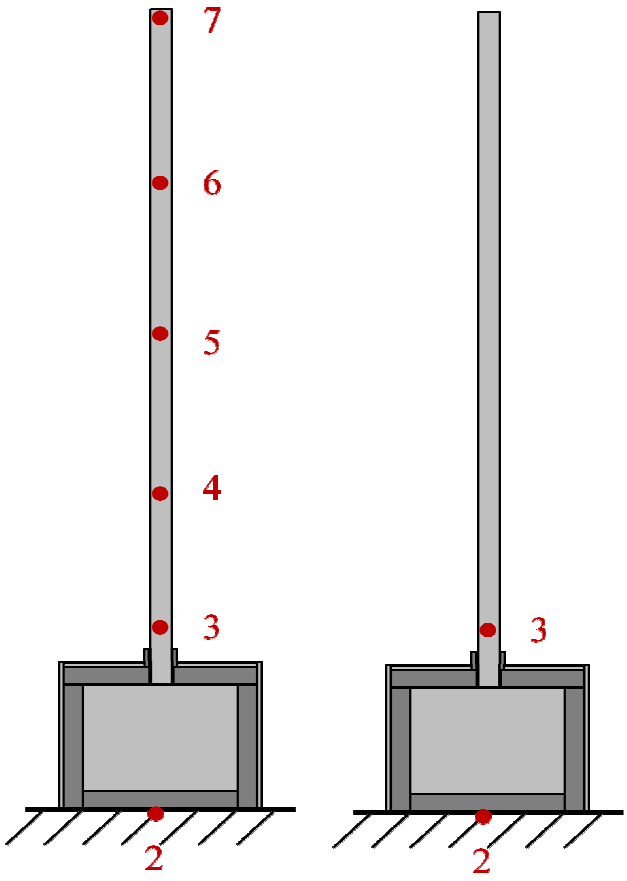

Figure 29: Accelerometer positions

4.4 Experimental Modal Analysis

Experimental Modal Analysis (EMA) was performed to identify the modal parameters (natural frequencies, mode shapes, and damping) of the system under consideration using measurements of the input and the output responses. In this case, the system is isolated from the environment, using soft materials such as sponge, and an impact hammer is used to generate an input signal, normally at a fixed location. The responses of selected points on the system are then measured using accelerometers. The frequency response function (FRF) was created from the information obtained from the input force and the output accelerations, from which the modal parameters can be found. FRF is simply a transfer signal function that can relate the output signal to the input signal in the frequency domain.

When the system is attached to complicated boundaries and vibration induced by random forces with unspecified locations, operated deflection shape (ODS) is used in this case to present an idea about the deflected shape of the structure under the effect of the operational load. One example of operational load is the vibration caused by the traffic on a bridge. In this work, the operational loads were simulated using earthquake simulations performed using computer software designed specifically for the University of Iowa by ANCO Engineers using a simple one-degree-of-motion shake table (Figure 30).

Figure 30: Shake table

More specifically, Kobe earthquake signal was used to replicate the vibrations that the sign might feel while operational. During the experiment three different Kobe signals were used, North-South, East-West and UD. A small section of such a signal can be seen in Figure 31.

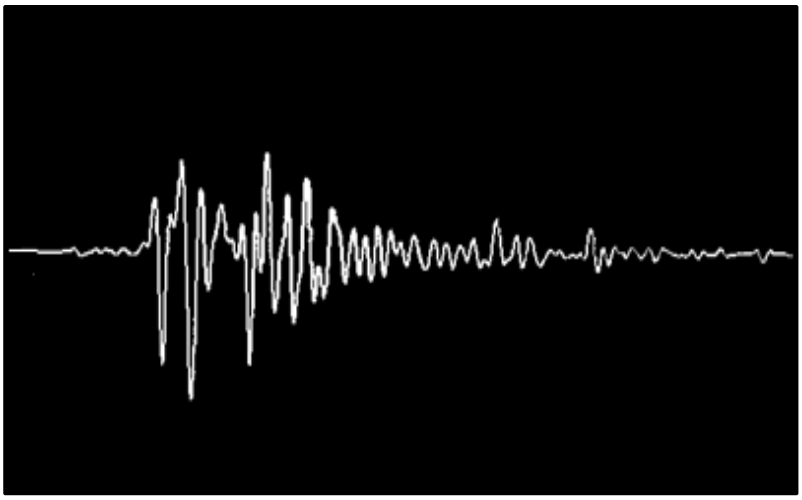

Figure 31: Kobe signal

In order to complete the EMA Easy Analyst and ME'scope software had to be utilized. The experimental analysis required for operating deflection shapes (ODS) to be determined using Easy Analyst software, after which the data was transferred to ME'scope and analyzed. ODS is a method used to animate the structure under operational loads such as the earthquake signals of this work and measure the shape of the structure under these loading conditions. When the excitation frequency gets closer to the natural frequency of the system the resulting shapes do not represent the mode shapes of the system but something very close to that. The idea behind ODS is to give general perception on how the structure is moving during the operation. The required set up procedure for Easy Analyst was completed prior to the experiment date. The setup required to complete these tests can be seen in Figure 32.

Figure 32: Experimental setup

Accelerometers were placed at five different, equally spaced, locations on the pipe (Figure 33). One additional accelerometer was placed at the bottom of the structure to act as a reference point. Three earthquake simulations were conducted and a set of data was collected by averaging those results. In order to be able to evaluate the effectiveness of the damper all of the tests had to be repeated for the model with the damper, as well as the one without the damper.

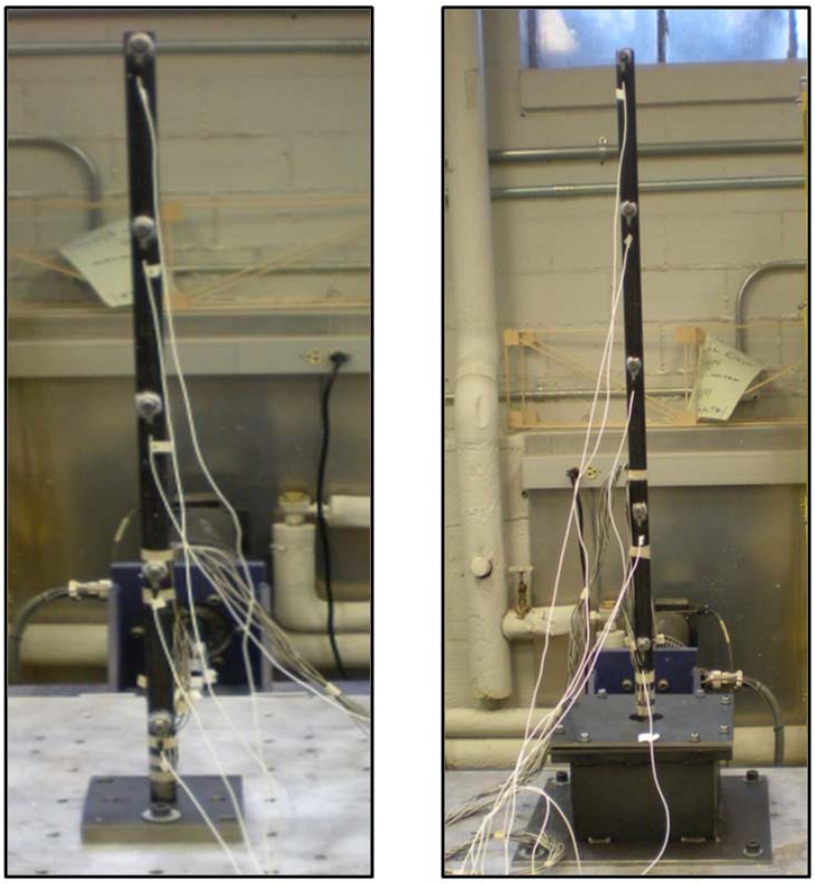

a. b.

Figure 33: Accelerometers
(a – no damper, b – damper)

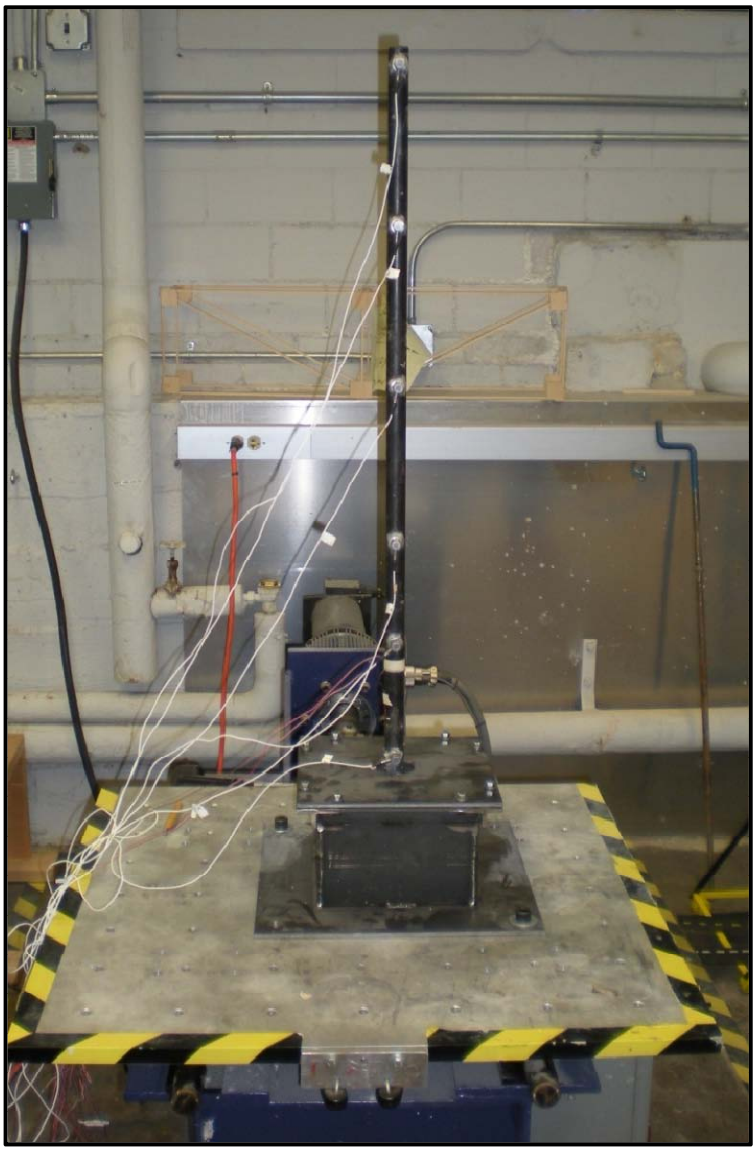

Figure 34: Damped structure on the shake table

The collected data was imported into *ME'scope* for processing and analysis. The auto-spectrum values were scaled and integrated. *ME'scope* is commercial software for structures which makes it easier to observe and analyze vibration based problems. Along with frequency response function (FRF) values, the operating deflection shape (ODS-FRF) was determined by the program using the principles of Fast Fourier transform. FRF allows us to determine all of the modal parameters, including the frequency, mode shape and damping coefficient.

The processed data was assigned to the corresponding pipe connection points of a model created in the *ME'scope* workspace. All data was positioned in reference to the identified reference point. Once all the ODS data was assigned, the model was animated at several of the response frequencies near the lower end of the frequency spectrum. In particular, several simple modal responses were found to assist in comparison with theoretical finite element modal results.

4.5 Strain testing

The reason for the strain test is to quantify, as possible, the maximum magnitude of the bending stresses at the base of the sign using traditional strain sensors. In this case two strain gauges were installed one facing the direction of motion of the shaker table, and the second 90 degrees away as shown in Figure 35. Because the loading is only applied in the one direction, it was assumed that maximum strain would occur in the direction of the shaker movement. For precaution, and to check what happens with the side-to- side motion a second strain gauge was installed.

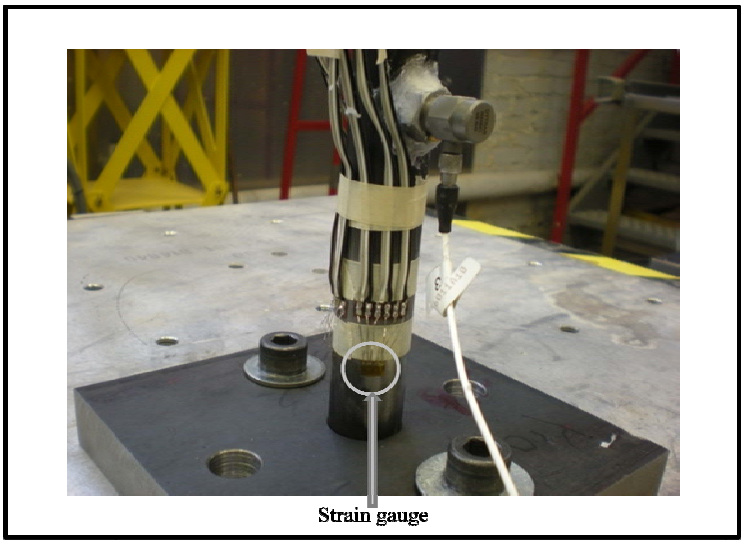

Figure 35: Strain gauges

Once the strain gauges were installed testing was performed using all three of the signals. Similarly to the modal analysis the signals were executed at different amplitudes, in this case at 40 and at the 80 percent of the signal. The results were then imported into Microsoft Office Excel and normalized.

4.6 Impact test

With the intention of comparing the undamped and damped results simple impact test was performed. For this test the accelerometers were placed on the pipe. The loading was applied on the tip point using a hammer. These results were used to analyze the damping percentage in the structure.

4.7 Wind test

In order to simulate the effects of the wind gusts blowing on the sign structures a simple pull down test was performed. The test was carried out by applying displacement (force) on the top of the pipe and letting go (Figure 36). Data was collected for both the undamped and damped cases. For this test all 6 accelerometers were placed on the sign structure. This data was analyzed in *ME'scope*.

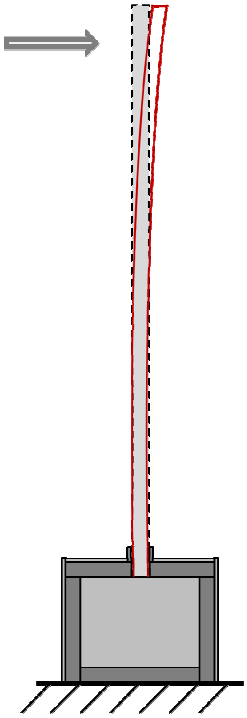

Figure 36: Wind test

4.8 Damping

One of the ways that the effectiveness of the damping device can be evaluated is by looking at the damping percentage of the structure. Each material has a natural damping percentage, for example steel has a damping percentage between 0.5 and 1 percent. However, the damping percentage of the structure is not only dependant on the materials used; it is also dependant on the connections. Determining the damping percentage for a complicated system is usually done by curve fitting the modal parameters of the FRF. Me-Scope has this capability built in (Figure 37). In addition to being able to estimate the damping percentage, curve fitting can also estimate residue.

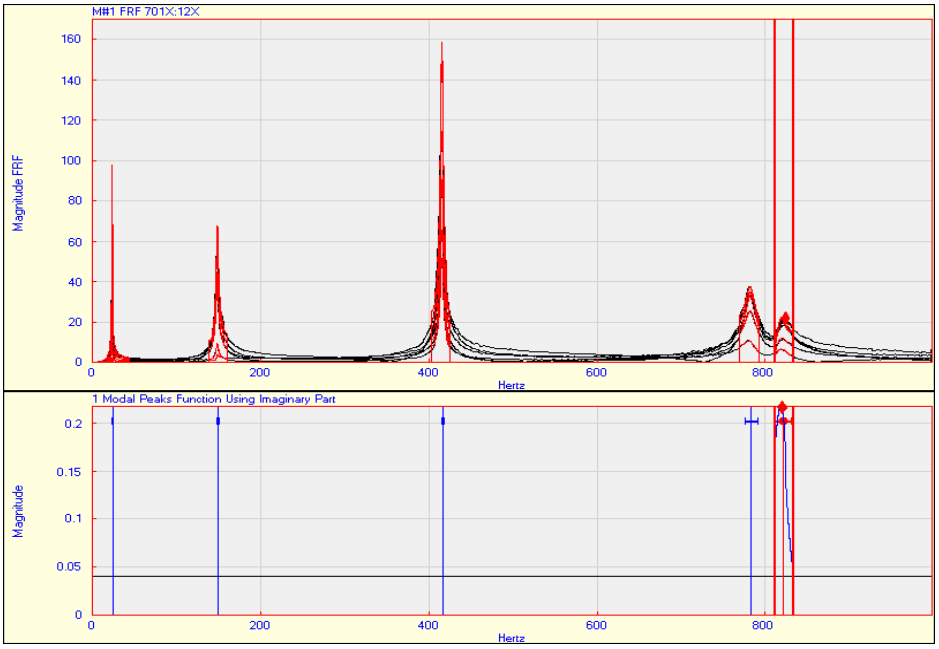

Figure 37: Modal parameters for undamped Kobe_EW

CHAPTER V
RESULTS

The first step in this work was to quantify the natural frequency of the sign with and without the additional mass. Using ANSYS, the results for the first five natural frequencies is shown in Table 5. As expected, the additional mass has lowered the natural frequencies of the system. The natural frequency of the system was also found using the experimental modal analysis techniques. The results for the experimental modal analysis are demonstrated in Table 7. It can be seen from Table 6 and Table 7that the experimental results are in close agreement with those obtained using ANSYS.

For the ground excitation tests, the results for the undamped Kobe_EW30 have shown that the maximum reported frequency peak was 24 Hz with amplitude of 0.118 g (Figure 15a). In addition, several smaller frequency peaks were captured between 0 and 10 Hz. Those had a significantly smaller amplitude, less than 0.01 g. For the damped Kobe_EW30 signal, the largest frequency peak captured was at 23 Hz. Its amplitude was about 0.044 g (Figure 15b). Just as in the case of the undamped system, smaller frequencies with small amplitude were reported between 0 and 10 Hz. When the experiment was ran using an undamped Kobe_EW80 the maximum frequency peak was at 24.3 Hz, with amplitude of 0.146 g (Figure 16a). Damped Kobe_EW80 reported maximum frequency peak at about 23 Hz with amplitude of 0.045 g. In the case of undamped Kobe_UD30 the largest peak reported was at 24.5 Hz, with amplitude of 0.11 g (Figure 17a). Damped Kobe_UD30 had the maximum frequency at 23.3 Hz with amplitude of 0.017 g (Figure 17b). For the test using undamped Kobe_UD80 maximum frequency peak occurred at 24.2 Hz, with amplitude of 0.225 g. When the damped Kobe_UD80 was used maximum frequency occurred at 23.4 Hz, with amplitude of 0.048 g. Both the cases for Kobe_UD30 and Kobe_UD80 reported some frequencies with considerably smaller amplitudes. The last signal used was Kobe_NS. In the case of

undamped Kobe_NS30 maximum captured frequency was at 24 Hz with amplitude of 0.18 g (Figure 19a). Damped Kobe_NS30 captured a frequency of 23 Hz with amplitude of 0.0375 g (Figure 19b). Undamped Kobe_NS80 maximum frequency was at 24.1 Hz. This frequency had amplitude of 0.21 g (Figure 20a). Damped Kobe_NS80 maximum frequency was at 22.9 Hz, with amplitude of 0.051 g (Figure 20b).

The results of the undamped wind test for the point close to the base of the pipe show that there is a mode like a mode shape at a frequency around 25 Hz with amplitude of 0.014 g. For the damped test the results have indicated a mode shape like at 25.1 Hz with amplitude of 0.0082 g.

Strain tests for the undamped Kobe_NS_40 showed the maximum strain of 33 μ. Damped Kobe_NS_40 showed the maximum strain to be at 25 μ. Undamped Kobe_NS_80 reported the maximum strain at 82 μ. Damped Kobe_NS_80 largest strain was 52 μ. Undamped Kobe_EW_40 largest strain of 51 μ. Damped Kobe_EW_40 largest strain was at 34 μ. Undamped Kobe_EW_80 reported the largest strain of 94 μ, where as the damped case had the largest strain at 60 μ. Similarly, damped Kobe_UD_40 had the largest strain at 21 μ. Damped Kobe_UD_80 had the largest strain of 46 μ.

5.1 Ground motion tests

5.1.1 Whole pipe results

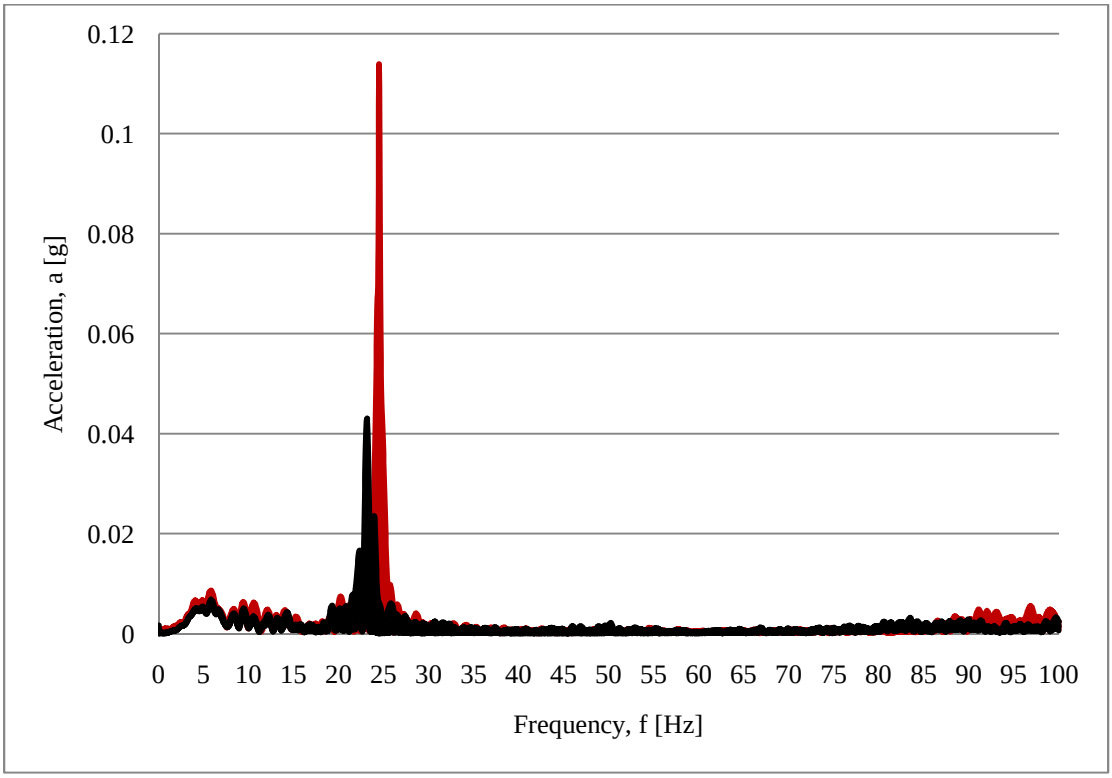

Figure 38: Operational Deflection Shape (ODS) result for Kobe_EW_30
(Red – undamped results, Black – damped results)

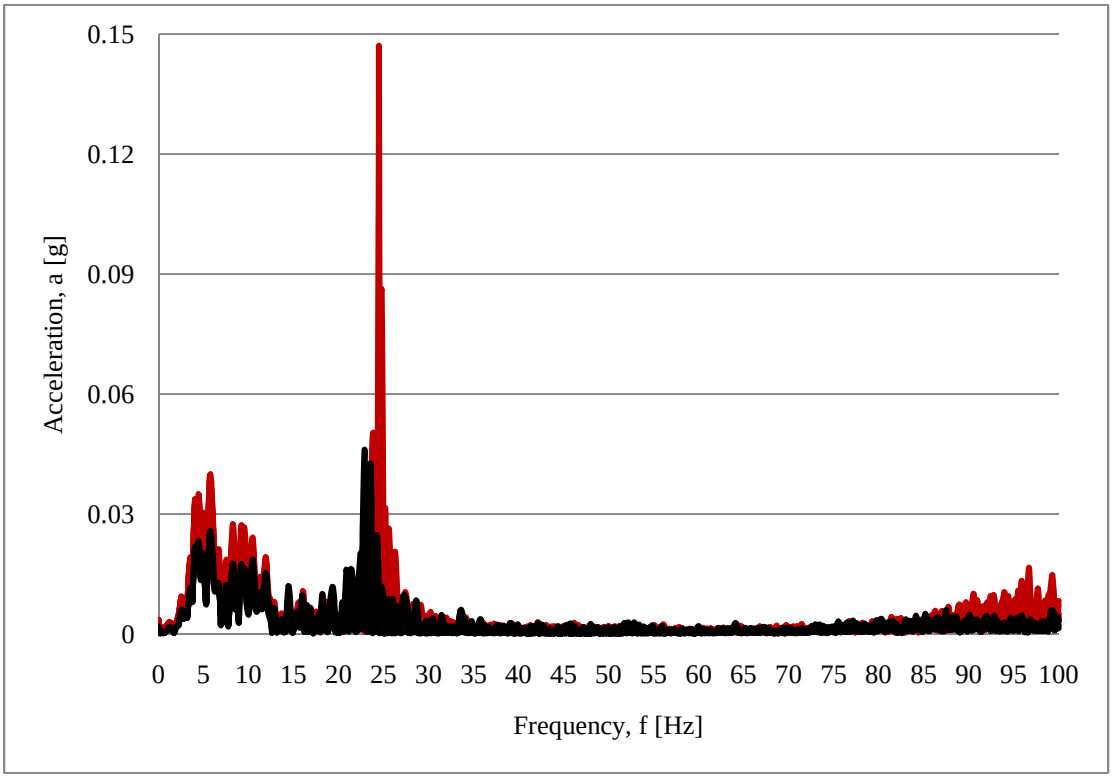

Figure 39: Operational Deflection Shape (ODS) result for Kobe_EW_80
(Red – undamped results, Black – damped results)

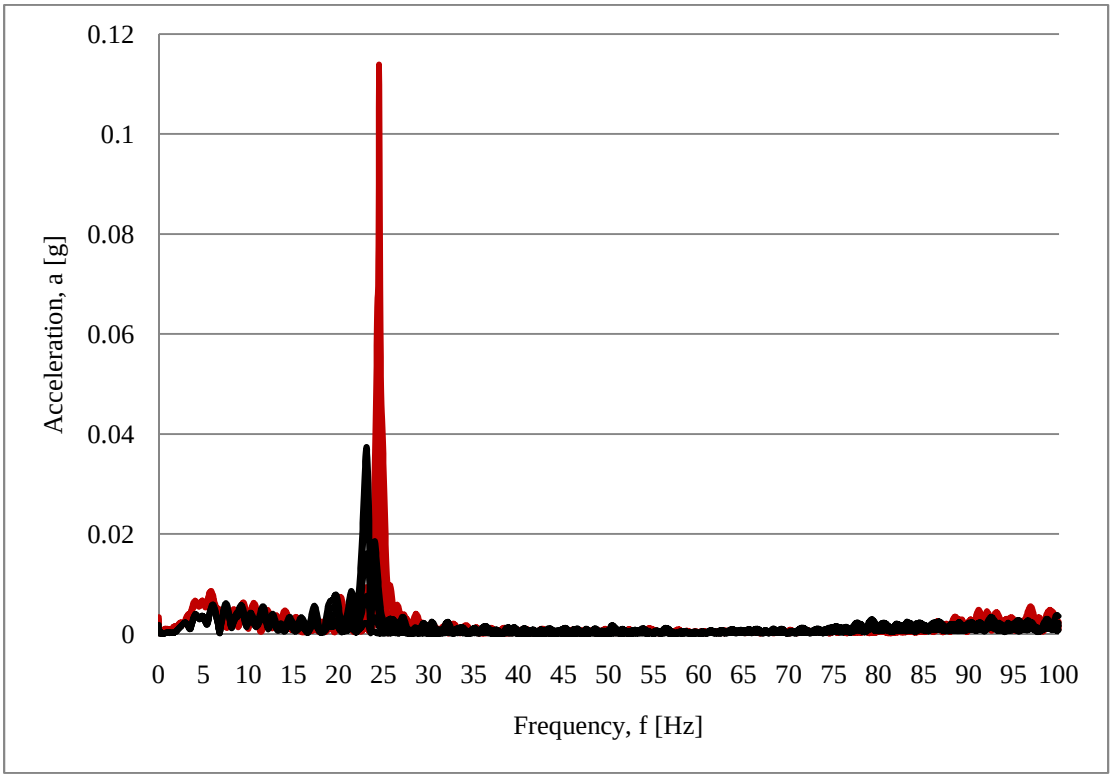

Figure 40: Operational Deflection Shape (ODS) result for Kobe_NS_30
(Red – undamped results, Black – damped results)

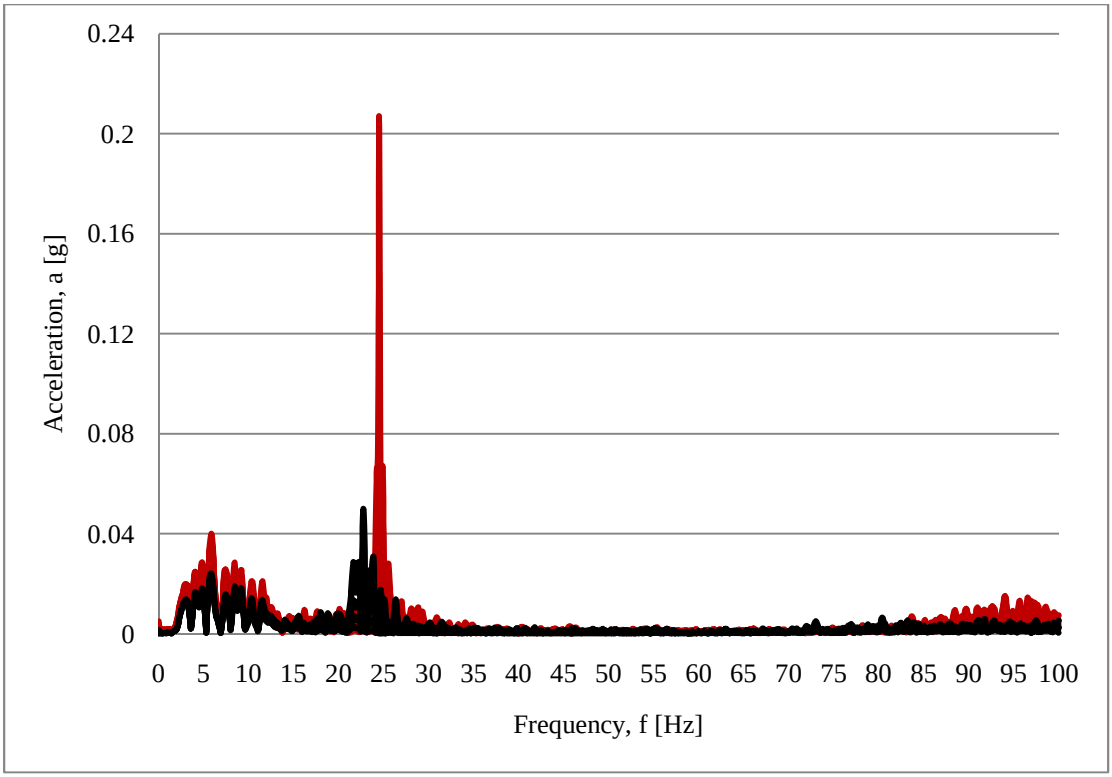

Figure 41: Operational Deflection Shape (ODS) result for Kobe_NS_80
(Red – undamped results, Black – damped results)

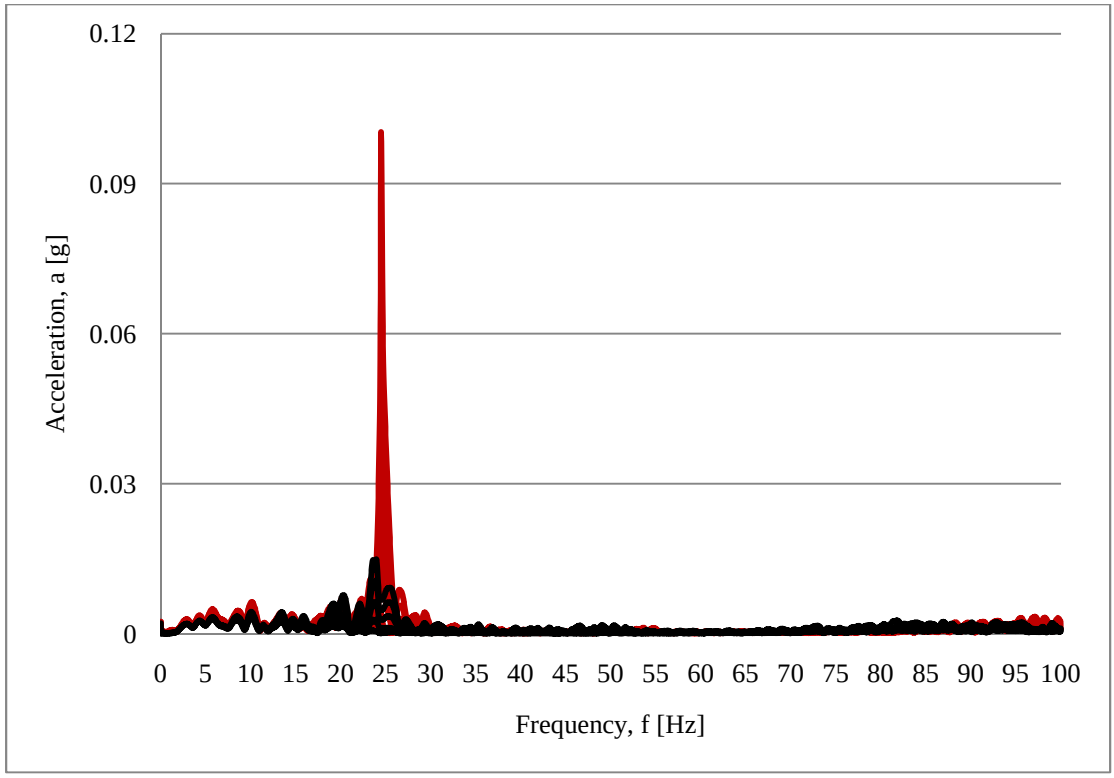

Figure 42: Operational Deflection Shape (ODS) result for Kobe_UD_30
(Red – undamped results, Black – damped results)

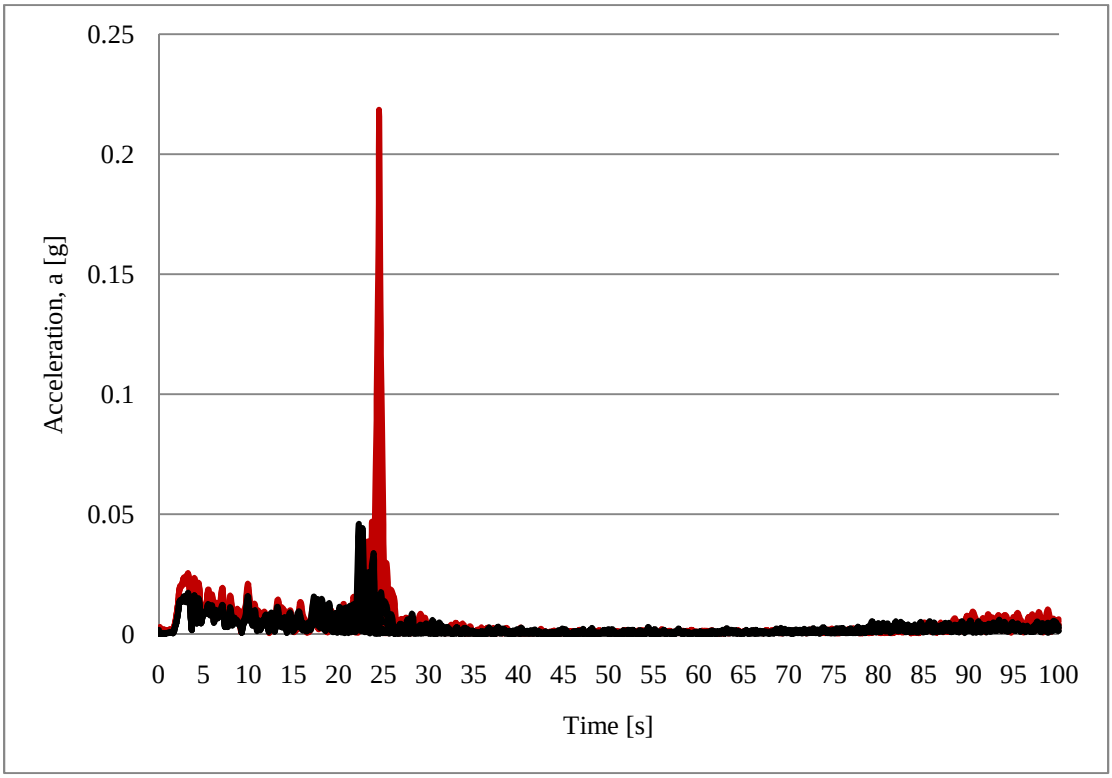

Figure 43: Operational Deflection Shape (ODS) result for Kobe_UD_80
(Red – undamped results, Black – damped results)

Table 7: ODS - whole pipe results summary

Signal	Undamped case		Damped case		Percent Difference in Acceleration
	Peak Frequency [Hz]	Acceleration [g]	Peak Frequency [Hz]	Acceleration [g]	
EW_30	24.4	0.114	23.1	0.0425	62.72
EW_80	24.4	0.149	22.84	0.0462	68.99
NS_30	24.5	0.114	23	0.0369	67.63
NS_80	24.5	0.207	23.5	0.0491	76.28
UD_30	24.5	0.1	23.5	0.0139	86.10
UD_80	24.5	0.219	22.2	0.0439	79.95

Table 8: EMA Results

Modal shape	Frequency [Hz]		
	1 –M	10 - M	Fully damped structure
First mode	-	9	-
Second mode	25	24	24
Third mode	-	-	-
Forth mode	-	-	-
Fifth mode	-	-	-

5.1.2 Base point results

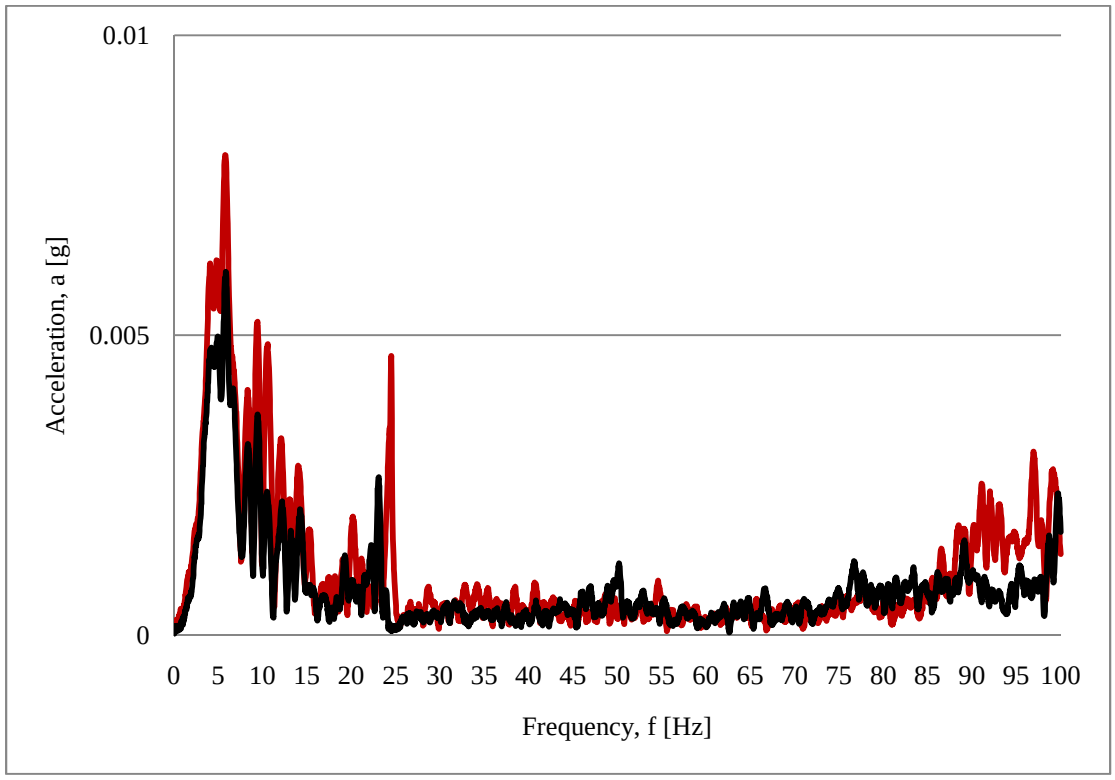

Figure 44: Operational Deflection Shape for Kobe_EW_30
(Red – undamped results, Black – damped results)

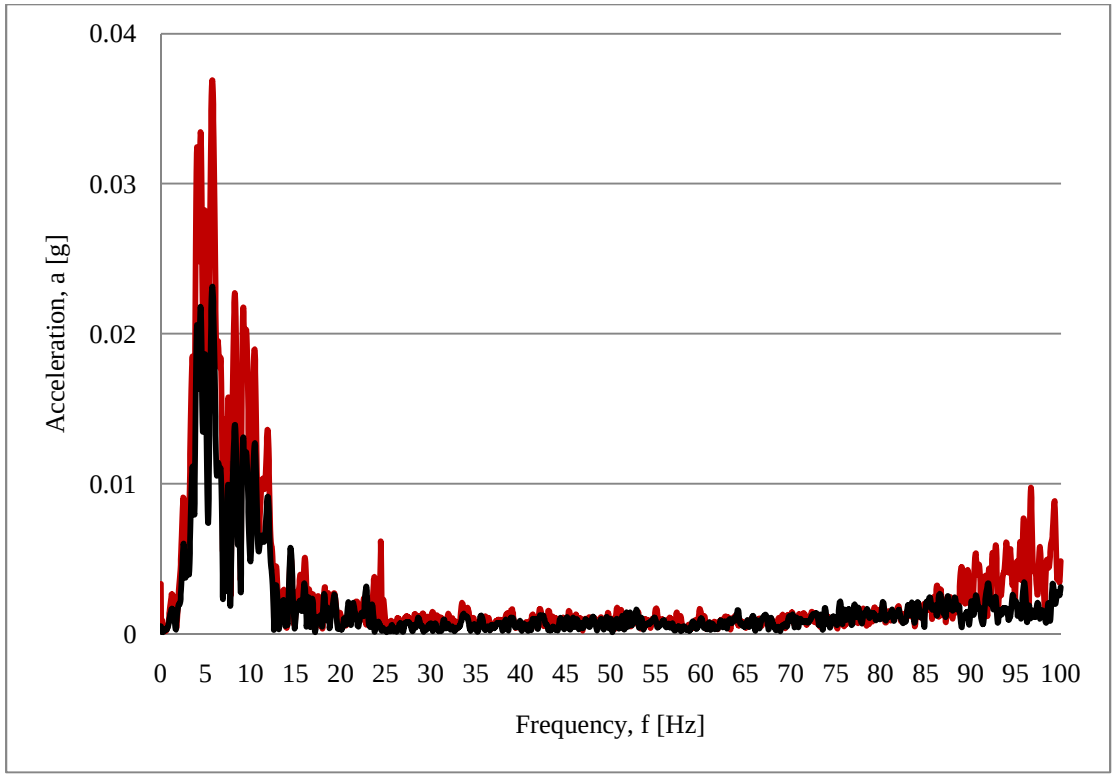

Figure 45: Operational Deflection Shape for Kobe_EW_80
(Red – undamped results, Black – damped results)

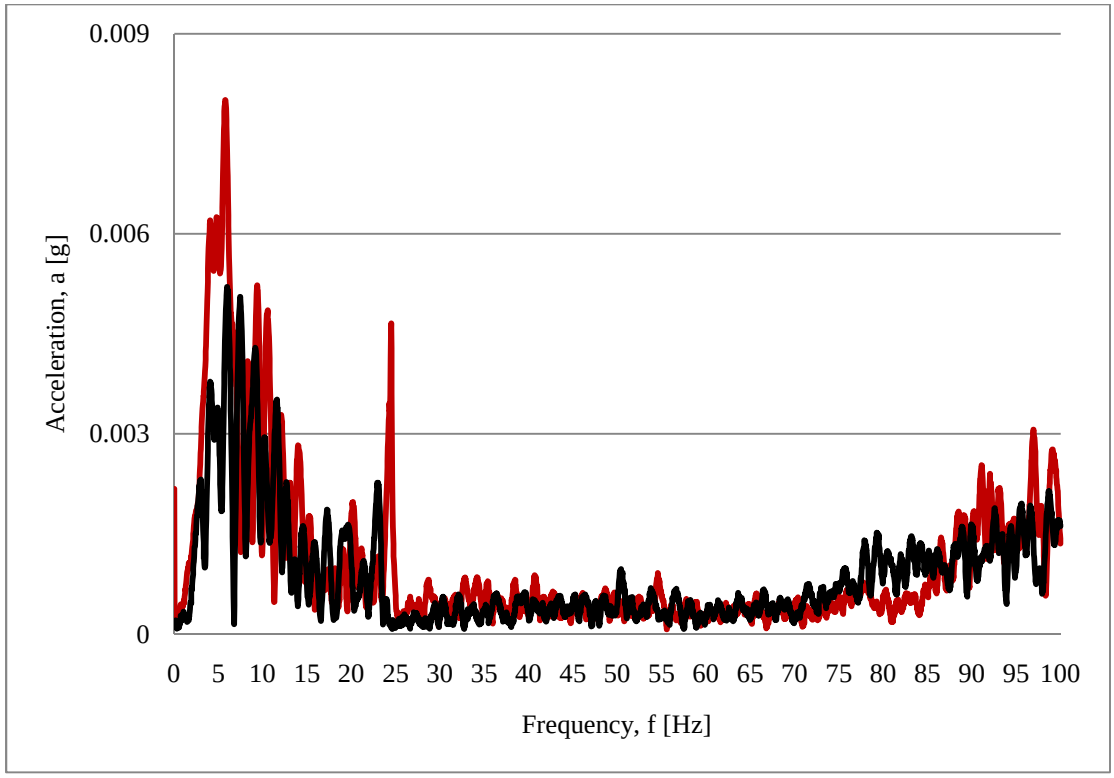

Figure 46: Operational Deflection Shape for Kobe_NS_30
(Red – undamped results, Black – damped results)

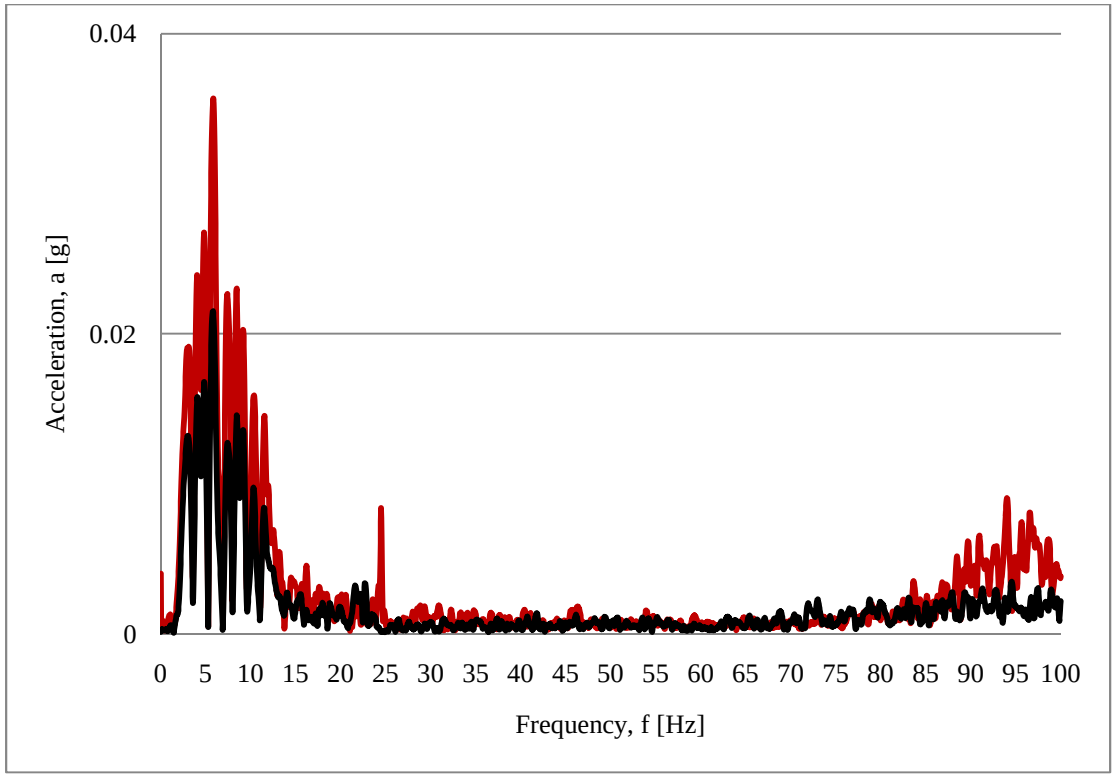

Figure 47: Operational Deflection Shape for Kobe_NS_80
(Red – undamped results, Black – damped results)

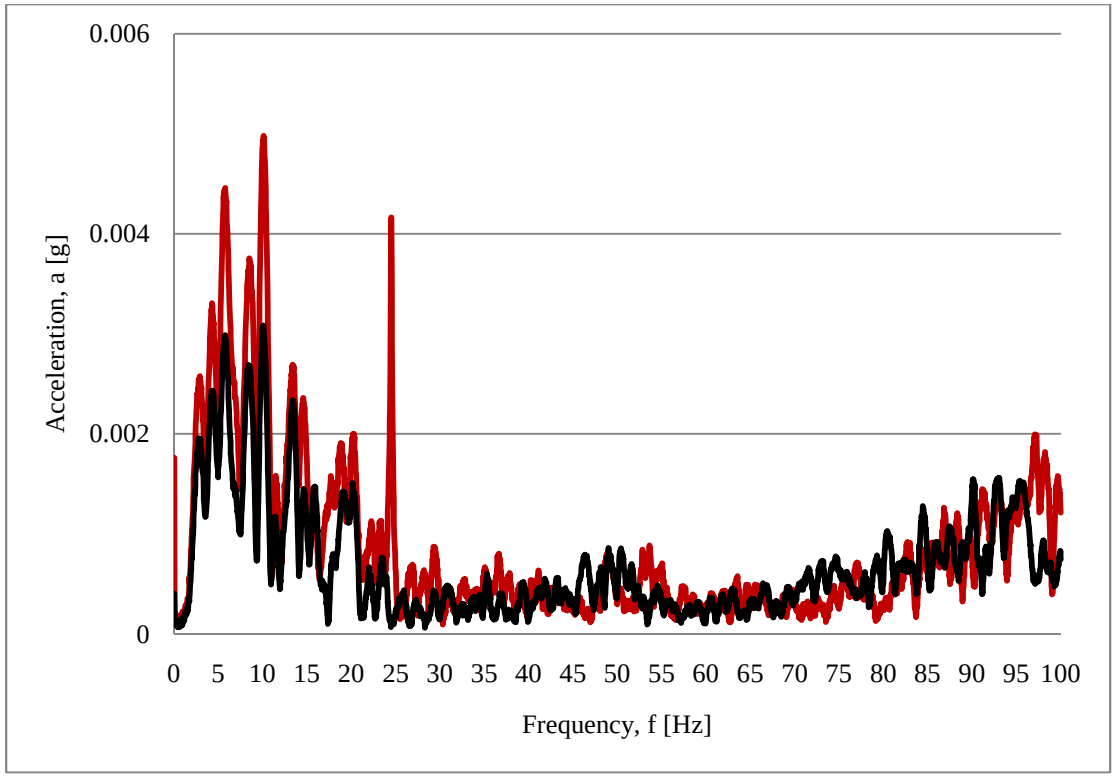

Figure 48: Operational Deflection Shape for Kobe_UD_30
(Red – undamped results, Black – damped results)

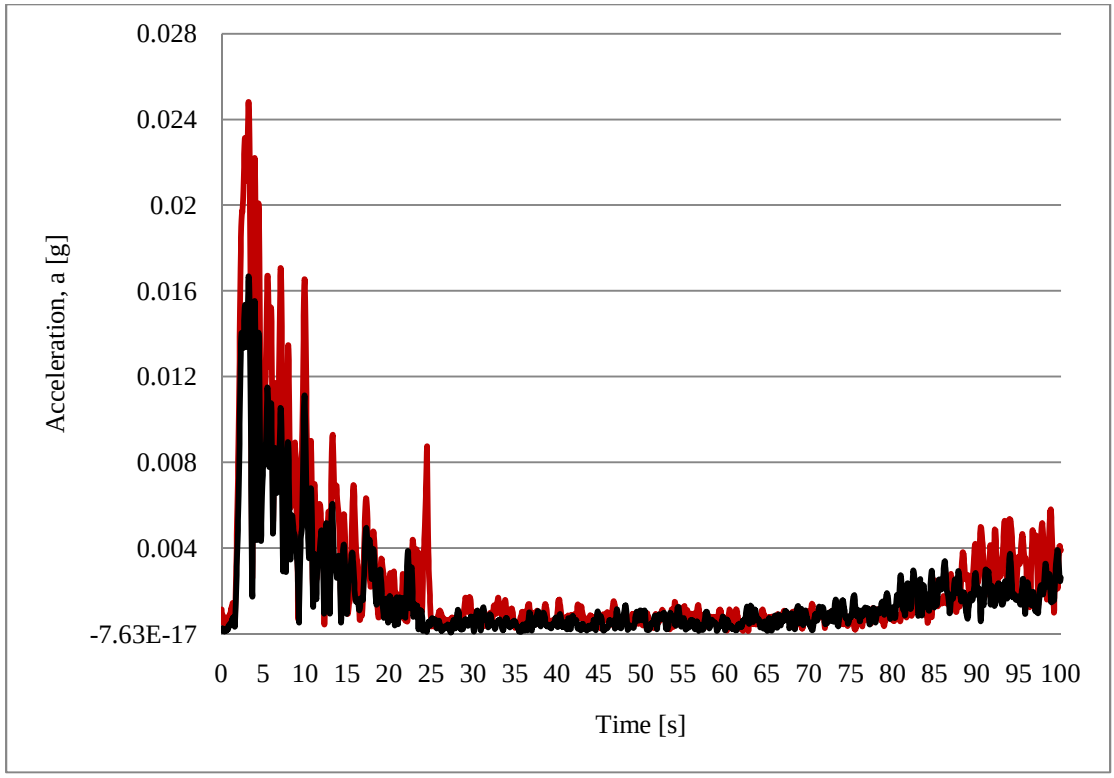

Figure 49: Operational Deflection Shape for Kobe_UD_80
(Red – undamped results, Black – damped results)

Table 9: ODS – base pipe results

Signal	**Undamped case**		**Damped case**		Percent Difference in Acceleration
	Peak Frequency [Hz]	Acceleration [g]	Peak Frequency [Hz]	Acceleration [g]	
EW_30	5.69	0.00791	5.81	0.00606	23.39
EW_80	5.69	0.0368	5.69	0.0228	38.04
NS_30	5.75	0.008	5.9	0.0052	35.00
NS_80	5.81	0.0357	5.75	0.0215	39.78
UD_30	10.09	0.00498	10.00	0.00308	38.15
UD_80	3.22	0.0248	3.22	0.0167	32.66

5.2 Wind test

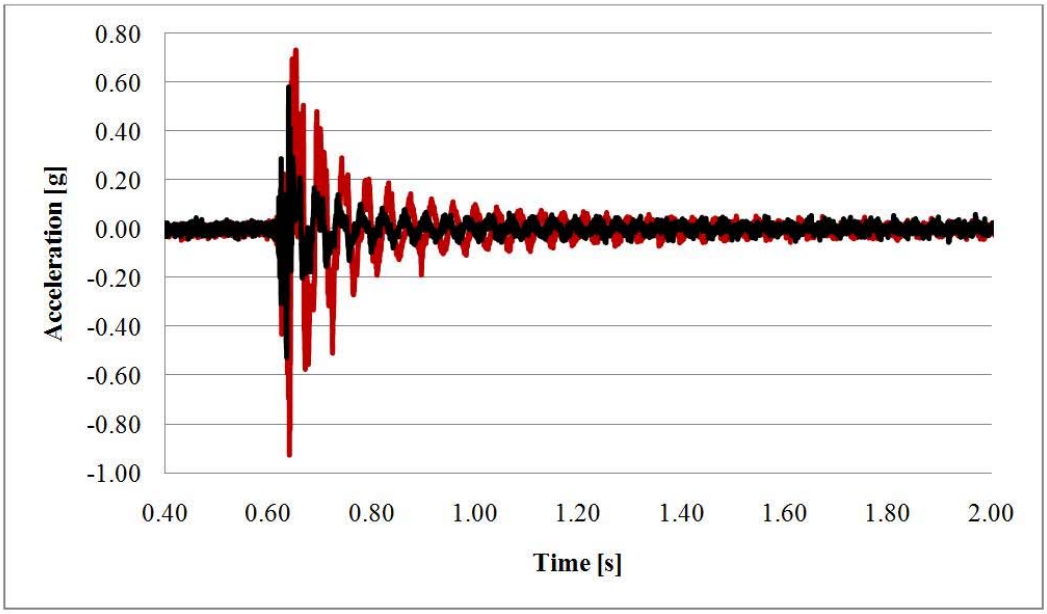

Figure 50: Time signal

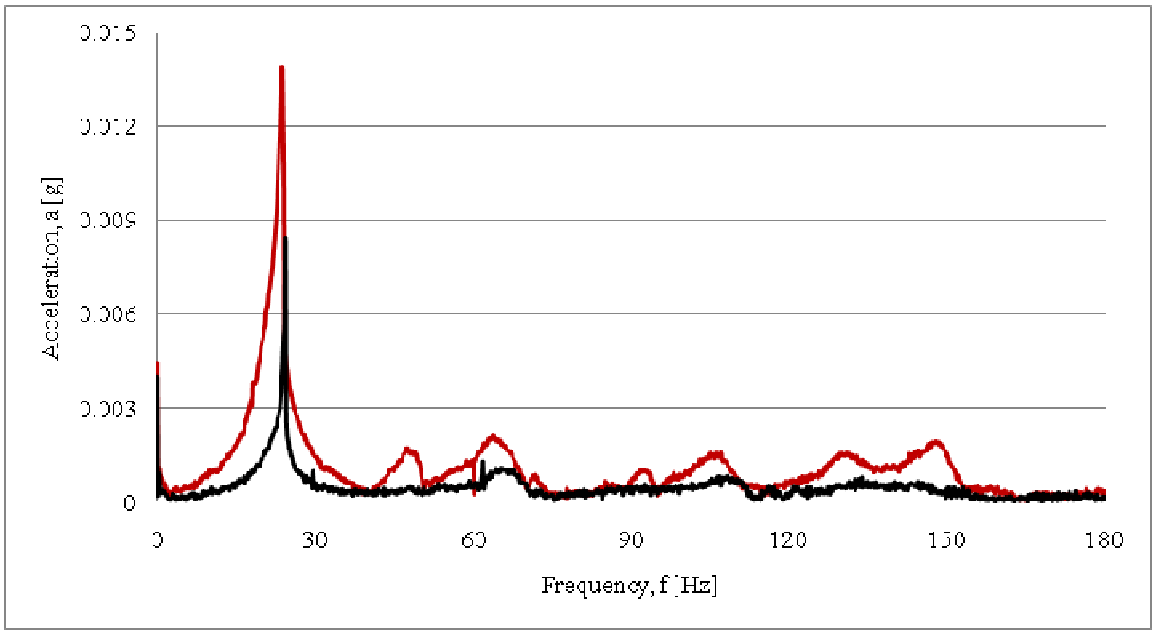

Figure 51: Operational Deflection Shape (ODS)
(Red – undamped results, Black – damped results)

Table 10: Wind test results

Wind test	**Undamped case**		**Damped case**		Percent Difference in Acceleration
	Peak Frequency [Hz]	Acceleration [g]	Peak Frequency [Hz]	Acceleration [g]	
	23.7	0.0139	24.4	0.00838	39.71

5.3 Strain test results

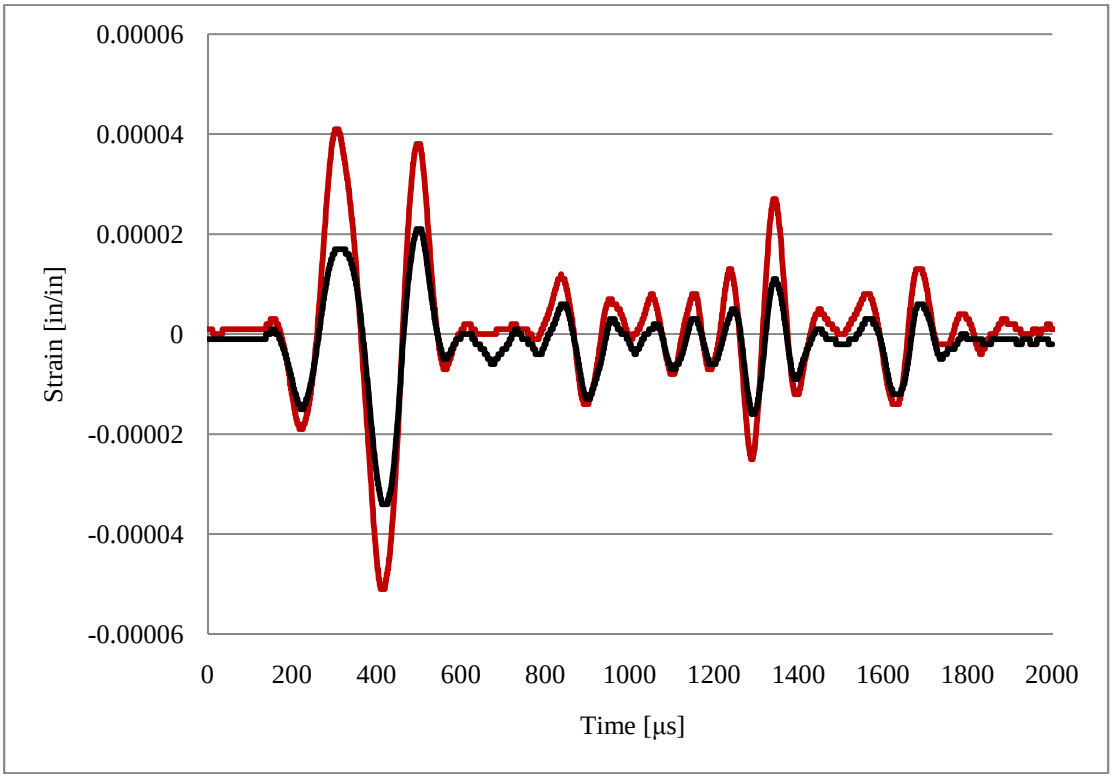

Figure 52: Strain test results for Kobe_EW_40
(Red – undamped results, Black – damped results)

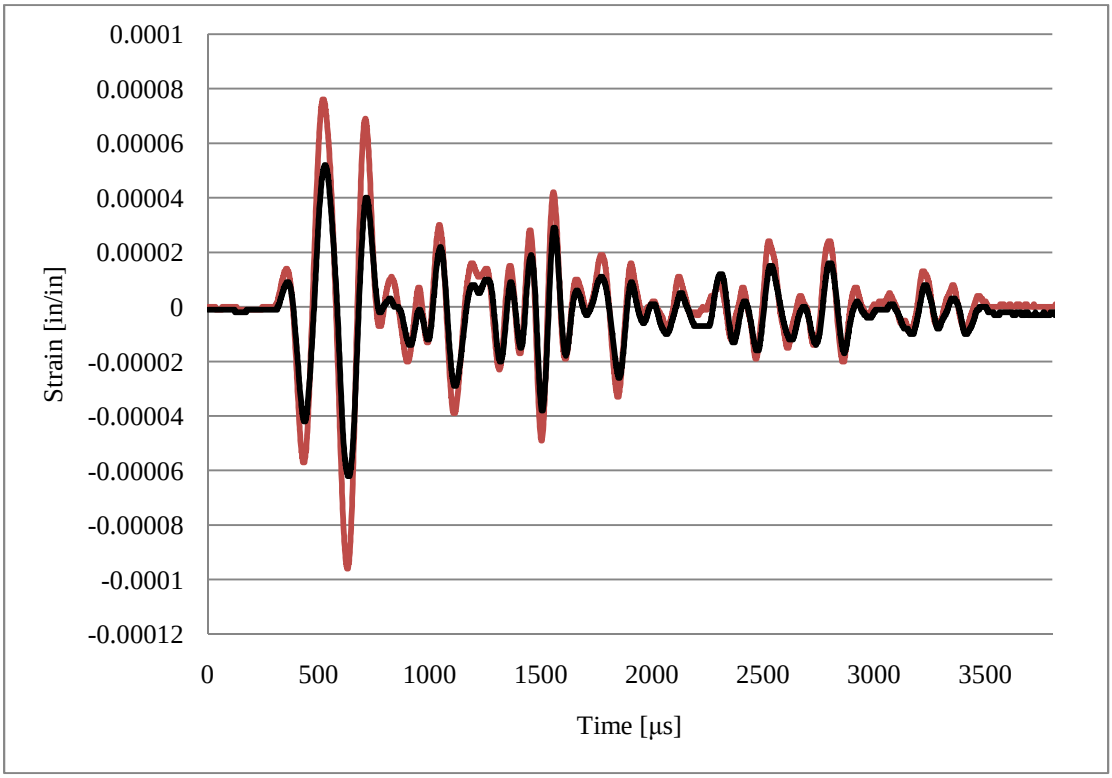

Figure 53: Strain test results for Kobe_EW_80
(Red – undamped results, Black – damped results)

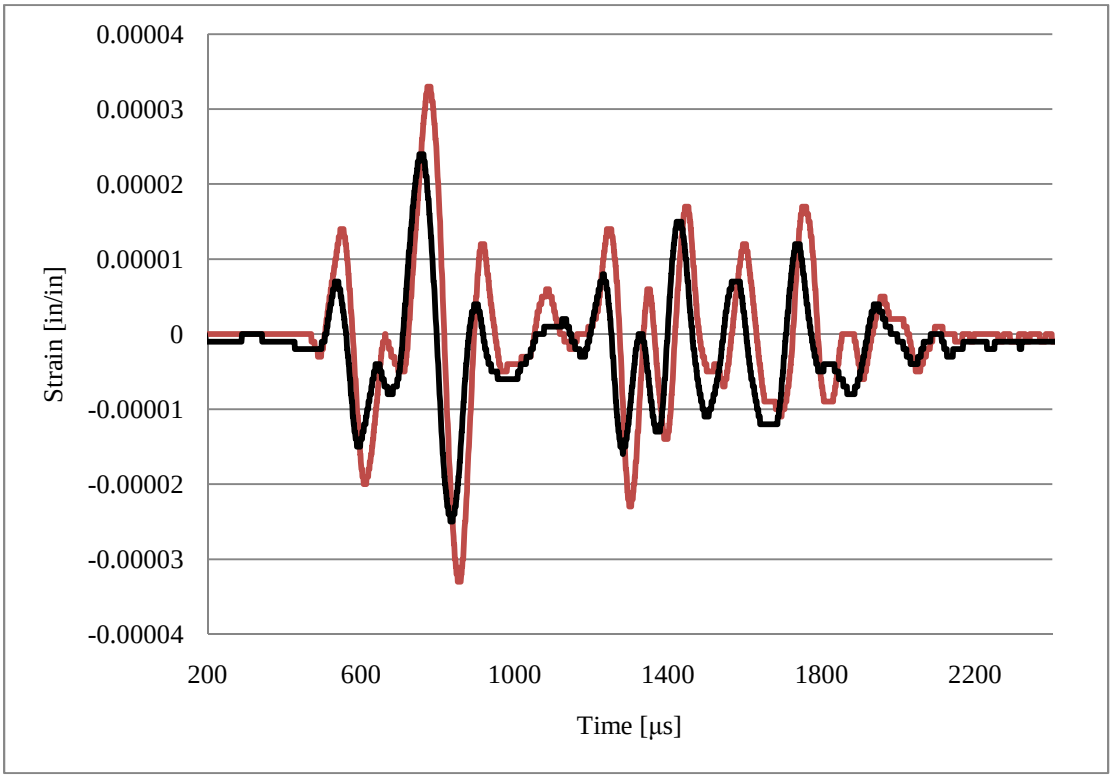

Figure 54: Strain test results for Kobe_NS_40
(Red – undamped results, Black – damped results)

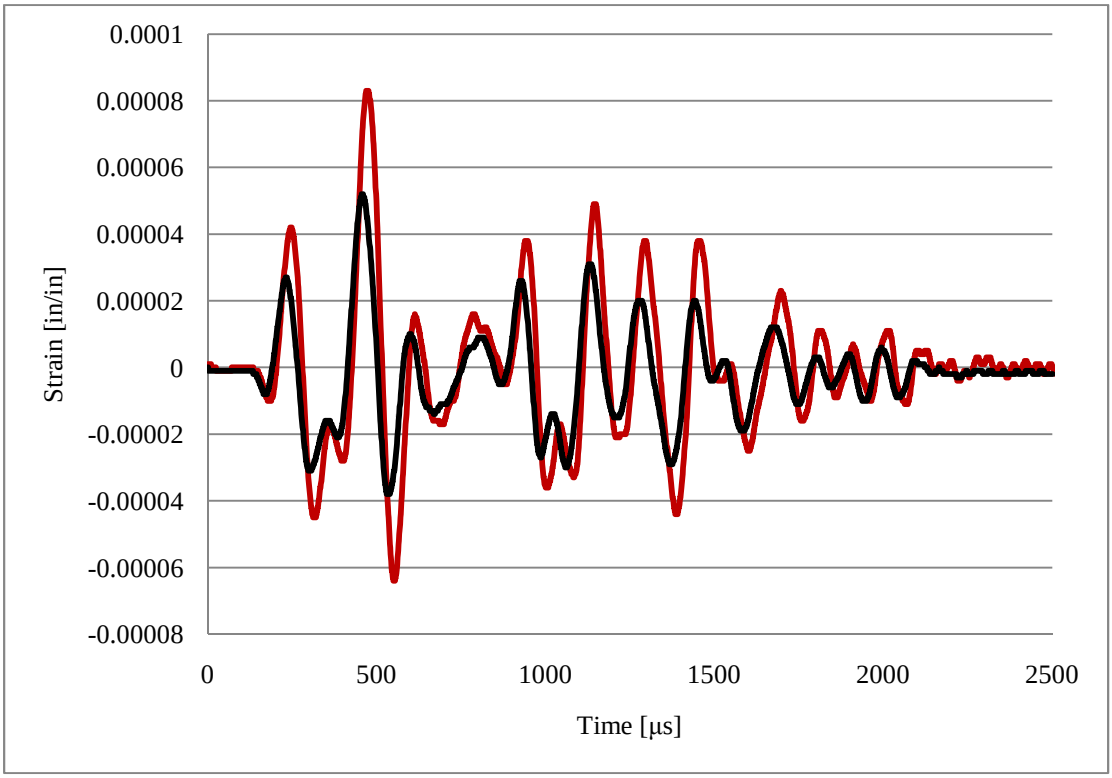

Figure 55: Strain test results for Kobe_NS_80
(Red – undamped results, Black – damped results)

Table 11: Strain test results

Signal	Un-damped		Damped		Percent Difference in stress
	Max strain	Max stress	Max strain	Max stress	
NS_40	33 μ	957 psi	24 μ	696 psi	27.3
NS_80	90 μ	2610 psi	52 μ	1508 psi	42.2
EW_40	51 μ	1479 psi	34 μ	986 psi	33.3
EW_80	96 μ	2784 psi	62 μ	1798 psi	35.4

5.4 Damping results

Table 12: Damping percentage results for the impact test

	Undamped results		Damped results		Percent difference in damping
	Frequency [Hz]	Damping (%)	Frequency [Hz]	Damping (%)	
Impact test	24.1	0.9	23.3	1.56	73.3
	149	0.84	153	2.12	152.4
	417	0.353	424	0.625	77.1
	804	0.148	800	0.41	177

5.5 Fast Fourier Transform (FFT)

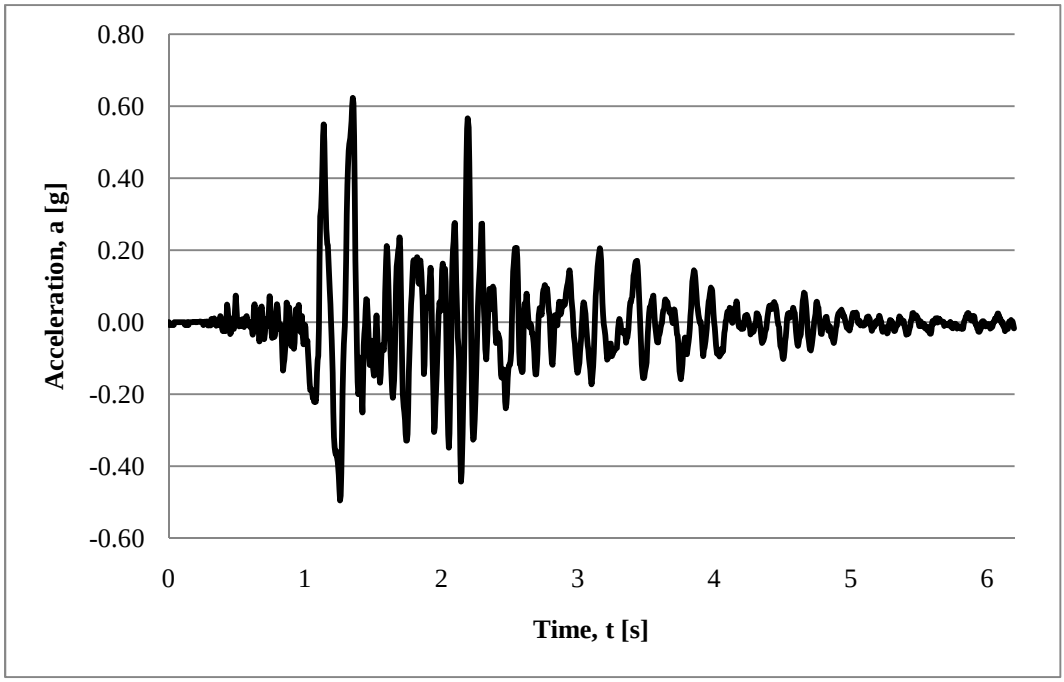

Figure 56: Kobe_EW signal

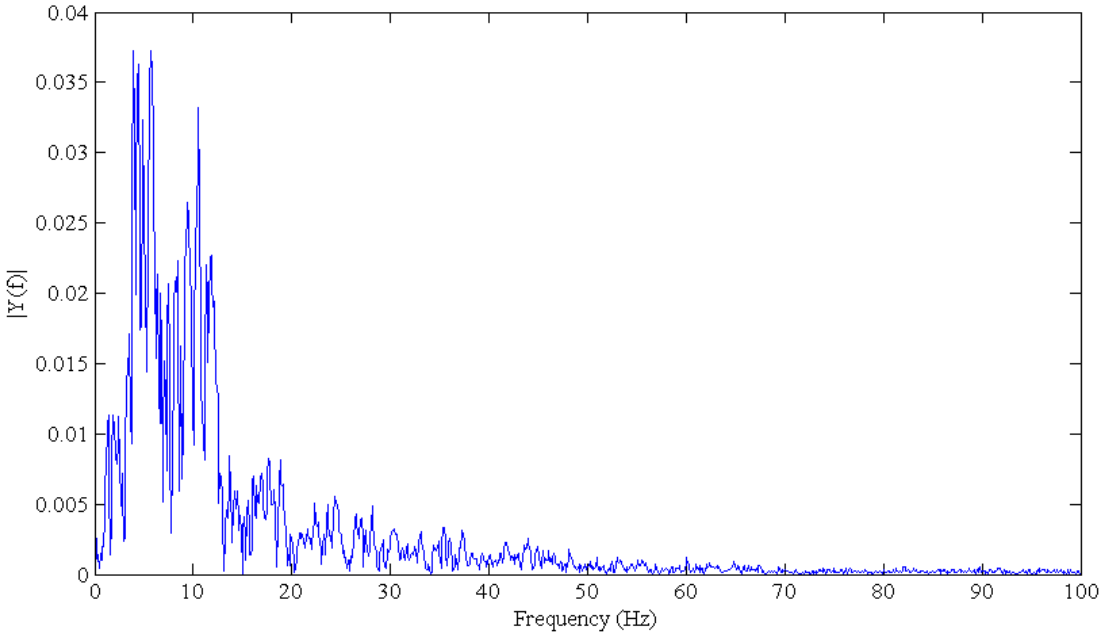

Figure 57: FFT for Kobe_EW

CHAPER VI
DISCUSSION

A passive mass-rubber damper was introduced in this work to be used as an integral part of highway traffic signs. The proposed damper has been designed to extend the life of the sign structure against three major sources of failure including bending, shear, and fatigue. The purpose of choosing the additional mass and installing it at the base of the sign was to decrease the natural frequency of the system, play as a restoring and stabilizing element against the ground motion, work to balance the system by bringing it center of gravity closer to the floor, and act as a low pass filter by having a flywheel effect. Still, the adding mass will have a negative effect and will increase the magnitude of the shear forces generated between the base of the system and the foundation. The rubber pads components of the damper will act to isolate the base of the sign from the ground and therefore, will absorb the energy resulting due to the relative sliding motion that causes shear. Therefore, the rubber will work on minimizing the shear forces on the base of the structure.

One of the main causes of failure in sign structure is bending. Bending failure tends to take place when the applied stress exceeds the yield strength of the material. During this work strain data was collected for several different tests. Hooke's law was used to calculate the corresponding stresses. Figures 38-43 and Table 7 show the effectiveness of the proposed damper in dealing with the bending problems. In this case the maximum stress was mitigated by up to 42 percent which would be significant for the cases of high winds or extreme ground motion. The strain results have also show similar behavior to the transmissibility results, by showing low strain magnitude at higher frequencies. Another notable finding was that the damper was more efficient when the applied loads were higher, making it very efficient for earthquake prone zones.

Failure in shear is one more common failure mechanism in sign structures. Shear force can be caused by both wind loading and ground motion. The damper was very effective in reducing the amount of the relative horizontal motion that causes the shear stresses. As can be seen from Figures 44-49 the magnitude of the relative acceleration has been decreased by up to 40 percent.

Another common failure mechanism in sign structures is fatigue. Generally, under normal wind loading sign structures experience high cycle fatigue. However in the case where resonance takes place low cycle fatigue can be expected. By using a damper some of this effect can be eliminated by shifting the frequencies and avoiding full scale resonance. The ODS results show, very clearly, the second resonant mode at around 24 Hz, which is a really close match to the natural modal frequencies calculated by the finite elements. This confirms the capability of the EMA to correctly predict the natural modal shapes.

The results have shown in general the ability of the proposed damper to achieve the design objective in terms of mitigating the energy entering the system due to ground motion and wind gusting. For the ground motion, Figure 35 shows the difference between the undamped and damped systems, where the magnitude of the ratio of the acceleration between the input and the output motion at the tip point is decrease by an order of three at the 24 Hz frequency. According to ANSYS modal analysis results and the EMA results, the 24 Hz represents the second natural frequency of the system. The damper has also affected the magnitude at the frequency of 8 Hz which represents the first natural frequency of the system. However, the damper performs much better around 24 Hz. The reason behind this behavior could be related to the choice of the magnitude of the base mass and the rubber materials. Looking back to the figure, we can see clearly the effectiveness of the damper at higher frequencies, where the figure show the diminishing effect of the higher frequency components of the signal. Mitigating the role of the higher

frequency components will have great benefit in minimizing the number of high frequency cycles that comprise the major components of the high cycle fatigue.

The results for the wind gust simulation have shown that the damper worked very effectively in mitigating the higher frequency components of the signal and in alleviating the magnitude of the effective signals by almost 46 percent.

Before the percent difference between the undamped and the damped systems can be evaluated it is important to note that some variation between the experimental and theoretical results was expected. This is because experimental modal analysis results show the response frequency to the load, while the theoretical analysis illustrates the natural frequency of the structure. If resonance takes place structure experiences large vibrations and displacements that often lead to failure. One of the most famous examples of this phenomenon occurred at the Tacoma Narrows Bridge. The bridge failed when the frequency of the wind load matched the natural frequency of the structure. This failure redefined the way that structural engineers look at dynamic loadings.

Additionally, a significant factor that cannot be ignored is damping. Each structure has internal damping that is a property of the material. For example, A36 steel has a standard coefficient of damping that ranges from 0.5 – 1 percent. Materials such as wood will have higher damping coefficients that range up to 20 percent. These factors must be considered in the modal analysis. In addition to the internal damping, the external supports can also introduce damping. Experimental modal analysis methods can be used to calculate this coefficient of damping. This is more important with models that are constructed from several materials where the interaction between these materials contributes a significant amount of damping.

For the sign structure tested damping percentage results, determined by curve fitting the FRF of the impact test, show that the damper increased the damping percentage by more than 70 percent for peak frequencies. Increase in damping can play a large role in minimizing moments in structures.

6.1 Conclusion

A low cost passive mass-rubber damper was introduced in this work to mitigate damage of highway signs caused by ground motion and wind gusting. The damper was designed and constructed to alleviate stresses due to bending, shear, and fatigue loading. Lab experiments based on sign responses and strains were conducted in order to evaluate the damper effectiveness in extending the life of the sign structure. Experimental Modal Analysis was performed to deduce the modal parameters of the structure using *Easy Analyst* and *ME'scope* commercial software. Ground motion was simulated using a shaker table and lighten earthquake signals. The wind gusting was simulated by simply pulling the tip of the sign and then releasing it. The result showed that the damper was very effective in filtering the high frequency components of the signals entering the system, minimizing by that failure due to high cycle fatigue. Strain results showed that the proposed damper was able to lower the maximum strain by up 46 percent. In addition, the results have shown that the proposed damper was able to minimize the horizontal relative ground motion between the base of the structure and the ground, which is an indication of smaller shear forces. Therefore, installation of this damper would increase the life a sign structure.

6.2 Future work

There are several improvements that could be incorporated to improve the effectiveness of the passive damper. To start with both the rubber and mass could be optimized. Additionally, cantilever sign structure could be tested to determine if the damper would still have similar capabilities in minimizing the effects of fatigue, bending and shear forces.

REFERENCES

1. Alexander, Louise and Wood, J. (2009) “A study of the low-cycle fatigue failure of a galvanised steel lighting column.” *Engineering Failure Analysis*, 16, 2153-2162

2. American Association of State Highway and Transportation Officials (AASHTO). (1994). *Standard Specifications for Structural Supports for Highway Signs, Luminaires, and Traffic Signals.* With Interims, Washington, D.C.

3. ANSYS version 11.0, (2007), (computer software), ANSYS Inc.

4. Campbell Technology Corporation. “Preemption”. Photograph. Campbelltechn.net. Web. 15 July 2010

5. Çelebi, Mehmet. Seismic Instrumentation of Buildings. USGS: Menlo Park, CA, April 2000.

6. Chan, Lok Shun. “Transmissibility.” Web. 20 June 2010. <http://personal.city.edu.hk/~bsapplec/transmis3.htm>.

7. Chthreepo. “Golden Gate Bridge”. Photograph. *Chreepo.com*. Web. 01 June. 2010.

8. Collins, T. J and Garlich, M. J. (1997) “Sign structures under watch.” Road and Bridges, July, pp. 38-44

9. Desai, Nihar and Yuan R. “Investigation of Bending/Buckling Characteristics for FRP Composite Poles”. (2006). ASCE

10. Dexter, R.J and Ricker, M. J. (2002) “Fatigue-Resistant Design of Cantilevered Signal, Sign and Light Supports”. *National Cooperative Highway Research Program (NCHRP) Report 469*, Transportation Research Board, National Research Council, Washington, DC.

11. Federal Highway Administration. *Sign Inspection*. U.S. Department of Transportation: Office of Bridge Technology

12. Fouad, H. “Impact of the new wind load provisions on the design of structural supports” (2002)

13. Gilani, A and Whittaker, A. (2000a) “Fatigue Life Evaluation of Steel Post Structures I: Background and Analysis.” *Journal of Structural Engineering*, 126 (3), 322-330.

14. Kasczinski, M. R. Dexter, R.J and Van Dien, J.P. (1998) “Fatigue-Resistant Design of Cantilevered Signal, Sign and Light Supports”. *National Cooperative Highway Research Program (NCHRP) Report 412*, Transportation Research Board, National Research Council, Washington, DC.

15. Mathematica version 7.0 (2009), (computer software), Wolfram Research

16. Me’ scope, (computer software), Vibrant Technology Inc.

17. US Department of Energy. “Wind powering America”. Photograph. Windpoweingamerica.gov. Web. 15 July. 2010.

18. Seismic Isolation Engineering, Inc. 9 Jan. 2007. Seismic Isolation Engineering, Inc. 3 May 2009.

19. Schwarz Brian, Richardson M. “Measurements Required for Displaying Operating Deflection Shapes.” *IMAC XXII Conference and Exposition on Structural Dynamics n.d. January 2004.* Vibrant Technology Inc. Web.

20. Stephens, Ralph, et al. *Metal fatigue in engineering – 2nd edition*. USA: John Wiley & Sons, 2001

21. Wikipedia. “*Golden Gate Bridge”*. Photograph. *Wikipedia.org.* Web. 01 June. 2010.